Incorporating cross-shore dynamics in ShorelineM for the long-term development of Mangrove-Mud coastlines

S. Potman

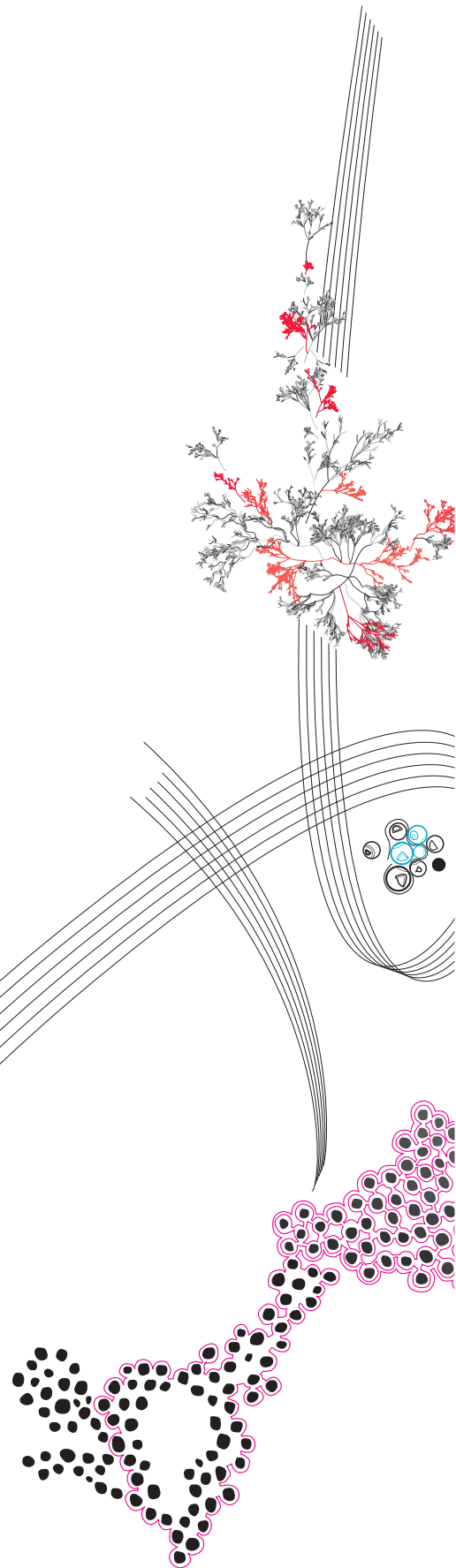Daily supervisor: Dr. Ir. E.M. Horstman

UT supervisor: Dr. Ir. P.C. Roos

External supervisor: Dr. Ir. J.T. Dijkstra

December, 2024

UNIVERSITY OF TWENTE.

Deltares

Summary

Mangrove forests around the world play a crucial role in creating resilience to climate change and in sequestering carbon. The mangrove forests stabilize coastlines, reduce erosion, increase the biodiversity and protect people along the coast. The conditions of these forests are getting worse by human impacts (clearance and conversion) and impacts as erosion and inundation. In terms of area the mangrove forests lose terrain by these conditions (an area of 1.17×10^4 km^2 of mangroves is lost since 1996).

To model the long-term development of mangrove ecosystems, the transport and deposition processes of sediments around and within these ecosystems are important. The spatial distribution of the sediments needs to incorporated in a more realistic way in models, to better model the development of mangrove-mud coastlines for the long-term. A model that is used for modelling this long-term development is ShorelineM. By its relatively simple principles of gradient driven alongshore transport and its low computational costs, this model can supply fast simulations for the long-term longshore development of mangrove-mud coastlines. However, the model has shortcomings in the cross-shore fluxes and the representation of mangroves needs improvements.

To represent the forest dynamics in a more realistic way, cross-shore morphodynamics of mangrove forests and establishment, growth and mortality of vegetation should be included. This may be possible by incorporating the cross-shore mangrove growth model MFlat, which includes the sediment- and morphodynamics of mangrove forests and the establishment, growth and mortality of mangrove trees.

The goal of this study was to investigate the capability of incorporating cross-shore dynamics from MFlat into the 1D longshore model ShorelineM to model the long-term development of mangrove-mud coastlines.

The most important limitations in ShorelineM are: the cross-shore distribution and entrainment of sediment; the assumed cross-shore shape and the absence of changes of the shape of the cross-shore profile in the mangrove zone, which influences the tidal prism and the cross-shore fluxes. The cross-shore profile of the mangrove zone is a uniformly sloped area, whereas in reality convex-up or concave-up profiles are formed. These cross-shore dynamics (profile changes and fluxes) can be resolved by MFlat, in which the cross-shore dynamics can be simulated in a realistic way, which has already been shown at the Guyana coast.

In MFlat, the morphology of mangrove forests is growing towards an equilibrium state based on the given conditions, which is in this study reached after roughly 40 years (for constant boundary conditions and with no mangroves at the start of the simulation). For conditions with a high boundary sediment concentration ($c_{bcs} = 0.50$ g/l) and a low wave height ($H_{rms} = 0.10$ m), the mangrove- and mudflat width after 40 years is almost 3500 m (which is the model domain). For conditions with a low sediment concentration there is almost no mangrove development.

From MFlat, the equilibrium width after 40 years of simulating with different wave heights and sediment concentrations is used to inform ShorelineM. The development of the mangrove- and mudflat width in ShorelineM is based on the mangrove/mudflat width and

the simulation length of the MFlat simulations. Implementing the width of the mangrove- and mudflat area from MFlat-simulations into ShorelineM improves the development of the mangrove- and mudflat width and capability of ShorelineM to model the coastline development for 40 years. This is done for an idealized testcase at the Guyana coast with cyclic sediment conditions, and is compared to the original model with cyclic sediment conditions. However, as cross-shore dynamics are complex and include multiple processes, more morphodynamic processes should be implemented to further increase the model performance, such as incorporation of profile changes and a non-linear relationship of the development of the mangrove- and mudflat width. As in the current version, only a linear relationship of the development of the mangrove- and mudflat width is taken into account.

Implementing cross-shore dynamics from MFlat into ShorelineM in the way presented above, shows promising results and keeps the simulation time in ShorelineM low. With some extensions/ improvements (as a change of the profile shape) the model can be an useful tool for coastal planning.

Contents

Abbreviations

Abbreviation	Description	Unit
MHW	Mean High Water	m
MSL	Mean Sea Level	m
SLR	Sea Level Rise	m

Symbols

Symbol	Description	Unit
A	Nearshore cross-sectional area	m^2
b_2	Dimensionless growth parameter	[-]
b_3	Dimensionless growth parameter	[-]
B	Width of the foreshore area	m
B_f	Width of the mudflat area	m
B_{fm}	Width of the colonizing mangrove area	m
B_m	Width of the mangrove area	m
Bcs	MFlat parameter for sediment concentration at the boundary	g/l
C	Competition stress parameter	[-]
$\bar{c}$	Nearshore averaged sediment concentration	g/l
c	Sediment concentration	g/l
c_{bcs}	Sediment concentration at boundary of the MFlat model	g/l
C_d	Wind drag coefficient	[-]
c_f	Flow drag coefficient	[-]
d	Active profile height	m
D	Mangrove diameter	m^2
d_m	Tidal amplitude	m
D_{max}	Maximum mangrove diameter	m^2
$depo$	Deposition term	kg/m^{2}s
ero	Erosion term	kg/m^{2}s
E	Horizontal (Easting) axis for plotting of ShorelineM results	km
$F_{w,s}$	Wave forcing	N
g	Gravitational acceleration	m/s^2
G	Mangrove growth parameter	cm/yr
H	Mangrove height	m
h	Water depth	m
h_i	Water depth at cell i	m
H_{max}	Maximum mangrove height	m
H_s	Significant wave height	m
H_{rms}	Root mean square wave height	m
$H_{s,tdp}$	Significant wave height at the toe of the dynamic profile	m
I	Inundation stress parameter	[-]
L	Length of cross-shore profile MFlat	m
M	Erosion factor	kg/m^2/s
M_f	Morphological factor	[-]
n	Cross-shore coordinate ShorelineM	m
N	Vertical (Northing) axis for plotting of ShorelineM results	km
$p(n,s)$	Shoreline position with coordinates (n,s)	km

Symbol	Description	Unit
P	Tidal Prism	m^3
P_t	Hydroperiod	[-]
Q	Longshore discharge	m^3/s
Q_s	Longshore sediment transport	kg/m/s
Q_m	Cross-shore mud-flux	kg/m/s
q_m	Mud-flux towards mangroves	kg/m
q_{riv}	Mud-flux from rivers	kg/m
S	slope profile MFlat	m
s	Longshore coordinate ShorelineM	m
u_{10}	Wind velocity at 10 meters high	m/s
u_i	Cross-shore velocity at cell i	m/s
u_{rms}	Root-mean square orbital velocity	m/s
v	Longshore velocity	m/s
V_m	Volume of sediment in mangrove area	m^3
w_s	Fall velocity	m/s
x	Cross-shore distance MFlat	m
X_i	Distance from cell i to the land boundary	m
z	Bed level MFlat	m
ρ_b	Bulk density of sediment	kg/m^3
ρ_s	Density of the sediment	kg/m^3
ρ_w	Density of water	kg/m^3
ρ_a	Density of air	kg/m^3
τ	Shear stress	Pa
τ_c	Current-induced shear stress	Pa
τ_{cr}	Critical shear stress for erosion	Pa
τ_w	Wave-induced shear stress	Pa
$\tau_{w,s}$	Wind shear stress	Pa
$\bar{\tau}_{m,s}$	Longshore mean bed shear stress	Pa
ς	Factor for colonizing mangrove area extension	[-]
ϕ_c	Orientation of the shore normal with respect to North	deg
ϕ_{wind}	Angle of incidence of waves with respect to North	deg

List of Figures

List of Tables

1 Introduction

1.1 Background information

Mangrove forests around the world play a crucial role in creating resilience to climate change and in carbon sequestration (Global Mangrove Alliance, 2022). Mangrove forests stabilize coastlines, reduce erosion, increase the biodiversity and protect people along the coast (Global Mangrove Alliance, 2022). The forests regularly face tidal inundation and the trees in these forests possess physical adaptations to cope with the salt water present in the environment around their tissues. Additionally, their root systems have evolved to provide support in soft mud sediments and aboveground roots facilitate the uptake of oxygen from the atmosphere to their below-ground roots, primarily situated in anaerobic sediments (van Santen et al., 2007). Many mangrove species produce seedlings, while still attached to the parent plant. Some seedlings are then spread by water to new locations for colonization (Lewis, 2005).

Mangroves are situated along tropical coastlines with saline or brackish water. Figure 1 shows the distribution of mangroves in a world map as well as the number of mangrove species along each region 1 (Michel, 2014).
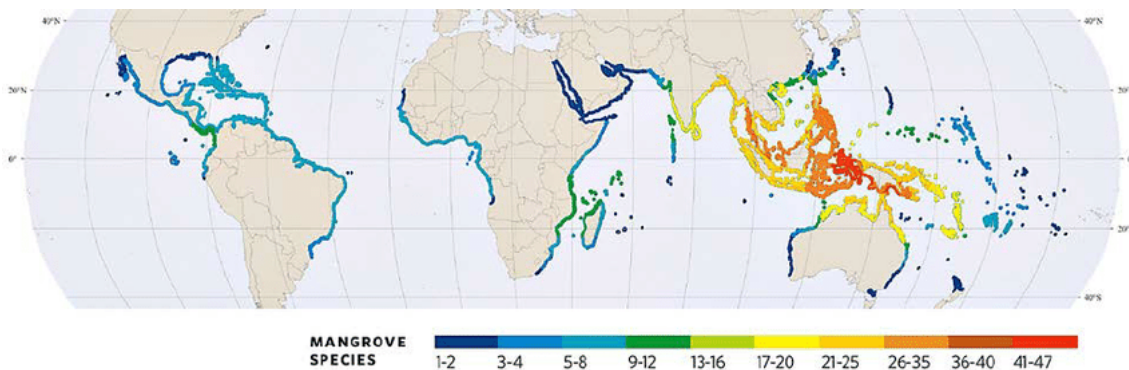
FIGURE 1: Distribution of mangrove forests over the world. The colors represent the number of species present in a certain region (Michel, 2014).

The zonation of mangrove forests is linked to factors such as tidal currents, elevation changes and salinity of the soil and water (Aluri, 2013). These factors influence the success of reproduction and the density properties of the forest. A typical zonation of mangrove forests is schematized in figure 2, where a division is made between lower- and upper coastal plain and the alluvial plain with different typical species that grow in each zone.
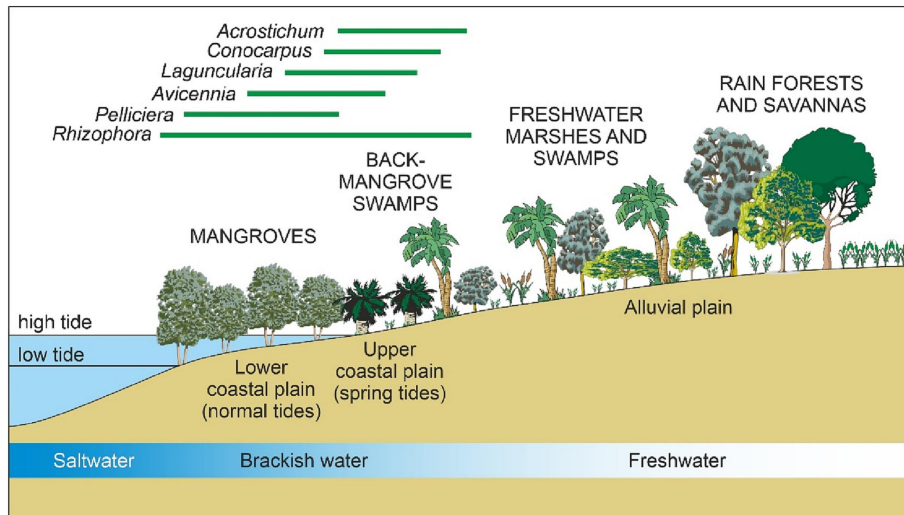
FIGURE 2: Typical zonation of a mangrove forest in the Caribbean. Per zone, the typical species that grow there are shown too (Rull, 2023).

Mangrove forests play a crucial role by stabilizing shorelines, attenuating wave and wind energy, and thereby defending coastal areas and structures (Horstman et al., 2014). The wave attenuation capacity of mangrove forests can vary over time, depending on the aboveground biomass, the hydrodynamics and the morphology in the forest and the development of the forests structure over time; see figure 3, where the attenuation capacity is given over time. During storm events, mangroves are damaged partly and extra sediment is transported into the mangroves. This extra sediment gives the mangroves the capacity to restore its morphology and vegetation if there is a surplus of sedimentation (Temmerman et al., 2023). If there is a deficit of sedimentation, the wave attenuation capacity of the mangroves will decrease over time. Mangroves also contribute to the support of coastal fisheries, by offering habitat and nourishment for fish and shellfish. Furthermore, these ecosystems hold diverse wildlife populations, including various birds (Lewis, 2005).
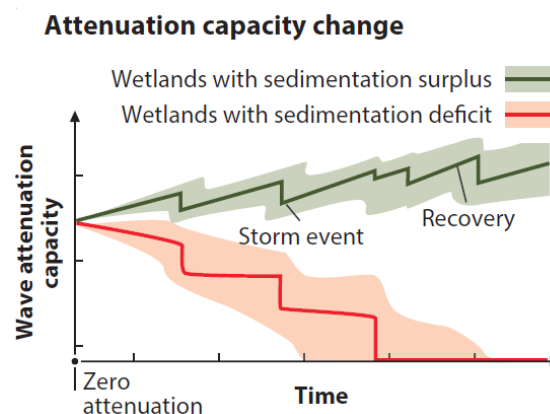
FIGURE 3: Evolution of wave attenuation capacity of mangroves in response to storm events (Temmerman et al., 2023).

To deal with the consequences of climate change (e.g. sea level rise, more extreme rainfall or storm events), there is an increasing interest in nature-based solutions for coastal defense (van Zelst et al., 2021). Mangrove forests are a nature-based solution for coastal

defense, present in the (sub)tropics, see figure 1. These mangrove forests can play an important role in mitigating the hazards induced by climate change (by stabilizing the coastlines and reducing erosion, which protects people along the coast), whilst also providing other ecosystem services such as carbon sequestration, fishery and habitat provision (Temmerman et al., 2023; van Zelst et al., 2021). Not only the present state of such ecosystems is relevant to coastal planning, but especially the expected development in response to stressors (e.g. reduction of sediment supply or increase in sea level) (Gijsman et al., 2021).

In response to these stressors the mangroves may lose their ability to protect coastal areas due to the relative elevation loss, which may result in a decrease in attenuation capacity and higher chances of flooding. These stressors may also result in lateral erosion of mangrove forests, which causes a loss of mangroves along the shoreline (Chan et al., 2024).

Importance of long term development

The living conditions of mangrove forests are getting worse by human impacts (clearance and conversion) and impacts as erosion and inundation, and in terms of area the mangrove forests lose a lot of terrain. The total area of mangrove forests was approximately 1.47×10^5 km^2 in 2022 (Bunting et al., 2022). Since 1996, an area of 1.17×10^4 km^2 of mangroves is lost over time, with average loss rates of between 0.26 and 0.66 percent per year (Hamilton and Casey, 2016). However, on some locations there were also improvements in the extent of mangrove forests, especially in river mouths and deltas. Yet, these improvements are not sufficient to contribute to a net increase of mangrove forests around the world (Bunting et al., 2022).

Modelling of long term development: ShorelineM and MFlat

To model the decadal development of mangrove ecosystems, the spatial distribution of sediments around and within these ecosystems is important. A model that is used for modelling this development is ShorelineM. By its relatively simple principles of gradient-driven alongshore transport and its low computational costs, this model can supply fast simulations (1-10 minutes) for the long-term development of the different zones of mangrove-mud coastlines (mudflat- and mangrove area) (Roelvink et al., 2020). However, the model has its limitations and the representation of mangroves needs improvements.

ShorelineM is a 1D longshore model created by UNESCO-IHE and Deltares, designed to simulate the position of a mangrove-mud coastline in response to wind and waves. The model incorporates sediment sources (e.g., rivers) and sinks (e.g., mangrove forests). It is an extension of ShorelineS, which is specifically designed for sandy coasts (Roelvink et al., 2020). In the model, mangrove forests face lateral expansion or erosion based on sediment fluxes into of out of the forests. The formulation of sediment fluxes and the representation of vegetation needs improvements, so that sediment and vegetation dynamics are represented in a more realistic way, with establishment, growth, and mortality of vegetation. This may be possible by incorporating the cross-shore mangrove growth model MFlat. This model was shown to reproduce stable and reliable results for a mangrove-mud coastline in Guyana and for a mudflat in the San Francisco Estuary (van der Wegen et al., 2019) and includes the cross-shore morphodynamics of mangrove forests and establishment, growth and mortality of mangrove trees.

MFlat is a process-based, morphodynamic profile model designed to investigate tidal and wave-induced morphodynamics on intertidal mudflats. It is an open-source Matlab

code that comprehensively describes both cross-shore and alongshore tidal hydrodynamics, including a stationary wave model (van der Wegen et al., 2019).

1.2 Problem Statement

ShorelineM focuses on assessing the longshore evolution of mangrove-mud coastlines in response to stressors like an increase in sea level rise or a decrease in sediment supply. Understanding these dynamics is essential for integrated coastal zone management of muddy coastlines where mud is stirred up by waves and currents. For the evolution of mangrove-mud coastlines, the sediment dynamics at mangrove forests are of great importance. They influence the forest dynamics (lateral- or surface accretion/ erosion) and therefore influence the long term development. However, these sediment dynamics are represented in a simplified way in the current version of ShorelineM (based on simple geometries). The sediment dynamics and spatial distribution of sediments needs to be incorporated in a more realistic way in models, to better model the development of mangrove-mud coastlines.

1.3 Research Goal

The goal of this research is to improve the capacity of ShorelineM, a 1D model for longshore mud-dynamics, to effectively simulate the decadal development of mangrove-mud coastlines. To this end, cross-shore dynamics and profile development must be incorporated in ShorelineM, so that the mud-fluxes into and out of the mangrove forest are represented better.

To effectively simulate the decadal mangrove development, the quantification of mud-fluxes into and out of the mangroves (cross-shore fluxes) and settling/erosion of the sediments has to be incorporated in the model. For the quantification of cross-shore fluxes the cross-shore mangrove growth model MFlat can be used. The cross-shore dynamics of mangroves in MFlat can be parameterized and incorporated in ShorelineM, to determine the long-term development of the mangrove forests in cross- and longshore direction.

To achieve this goal, the focus is on the cross-shore sediment transport processes (i.e. cross-shore fluxes, sediment trapping and erosion) that influence the long-term response. This research investigates the long-term response in 40 years of morphological evolution of the mangrove forest. This evolution has to be described in terms of the elevation of the mudflats and forests (bed level profiles), which determines the lateral expansion or erosion (shoreline evolution).

The simulations explore the responses on different stressors as a decrease of sediment supply or changing wind conditions with faster wind velocities.

1.4 Research Questions

To achieve the research goal, three research questions are formulated:

RQ1: How are current model assumptions in ShorelineM limiting the cross-shore development of mudflats and mangrove forests?

- How is the mangroves' morphology schematized in ShorelineM and how could this schematization be improved?

- How is the entrainment of sediment in the nearshore area schematized in ShorelineM and how could this schematization be improved?

- How are cross-shore fluxes computed in ShorelineM and how could this formulation be improved?

RQ2: How do the cross-shore profiles of mangrove forests develop on the long-term (up to 40 years) in the mangrove model MFlat for an idealized testcase in Guyana?

- What is the relation between variations in sediment concentration and wave height and the morphological development (mangrove width, tidal prism and sediment volume)?

- How are mud-fluxes distributed across the profile and how can the mud-fluxes to and from mangroves in MFlat be parameterized?

- What cross-shore dynamics from MFlat have to be parameterized for a realistic cross-shore development in ShorelineM?

RQ3: To what extent does coupling cross-shore dynamics from MFlat improve the longshore model ShorelineM for an idealized testcase in Guyana?

- How can the parametrizations from MFlat be implemented in ShorelineM to improve the capability of modelling mangrove development in ShorelineM?

- What is the difference between model results of the coupled model and the original model with simplified cross-shore fluxes at a schematized mudflat inspired by Guyana conditions?

1.5   Reading Guide

In Chapter 2, the methodology used during the thesis is presented, explaining how each of three research questions is answered. Chapter 3 then shows the results of simulations in ShorelineM and the possible improvements that can be made in the model to improve modelling the long term development of mangrove forests. Chapter 4 describes the equilibrium state in the cross-shore model MFlat, and shows the relation between sediment supply, wave height and forest width. Chapter 5 shows how the cross-shore dynamics from MFlat are implemented in ShorelineM and how simulations with this coupled model are different from simulations with the standard model. Finally, Chapter 6 contains the discussion and Chapter 7 the conclusions and recommendations.

2 Methodology

This chapter elaborates the methodology that is used during this thesis to answer the research questions. First, the two models that are used for the simulation of the long-term development of mangrove forests are explained: ShorelineM (§2.1) and MFlat (§2.2). The 1D longshore model ShorelineM has low computational costs, and can therefore easily be used to model the long term development of mangrove-mud coastlines for different hydrodynamic conditions (Roelvink et al., 2020). With the description of the model (§2.1) and additional simulations, research question RQ1 is answered. The cross-shore model MFlat includes cross-shore processes as erosion, sediment trapping and cross-shore fluxes that are missing in ShorelineM. With the description of the model (§2.2), the set-up (§2.3.3) and additional simulations, research question RQ2 is answered. Both models will be coupled, to increase the capability of ShorelineM to model the development of mangrove forests. To test this capability of the model, results of the model are compared to a field case in Guyana. With the set-up of the model (§2.3.2) and the schematization of the coupling (§2.3.5), research question RQ3 is answered.

2.1 ShorelineM

ShorelineM has been developed to model the evolution of muddy coastlines at monthly to centennial time scales. To model this evolution, the existing ShorelineS model (see Appendix A.1) has been extended and changed to the 1D mangrove model ShorelineM. This model consists of formulations that compute the longshore advection of mud and a component that simulates the position of a muddy coastline with areas where mangroves may grow. The cross-shore profile used for the formulations is presented in figure 4. This profile is a simplification of how the cross-shore profiles of mangrove forests look like in reality. As it only consists of two uniform linear slopes for the mangrove area (width B_m) and the foreshore area (width B). The mangrove area is the part of the coast that is between MHW and MSL, indicated by the tidal amplitude d_m. The foreshore area is part of the coast below MSL with an active profile height d. Between those two areas there is a mudflat area (width B_f) and a colonizing mangrove area (width B_{fm}), that colonizes parts of the mudflat area. The position of the cross-shore coordinate n is determined by the sum of the mangrove- and mudflat width. The volume of water that enters the (colonizing) mangrove zone is the tidal prism P, formed by MHW, the flat part of the colonizing mangrove zone and the sloping part of the mangrove zone. The tidal prism is visualized by the purple trapezium in figure 4.
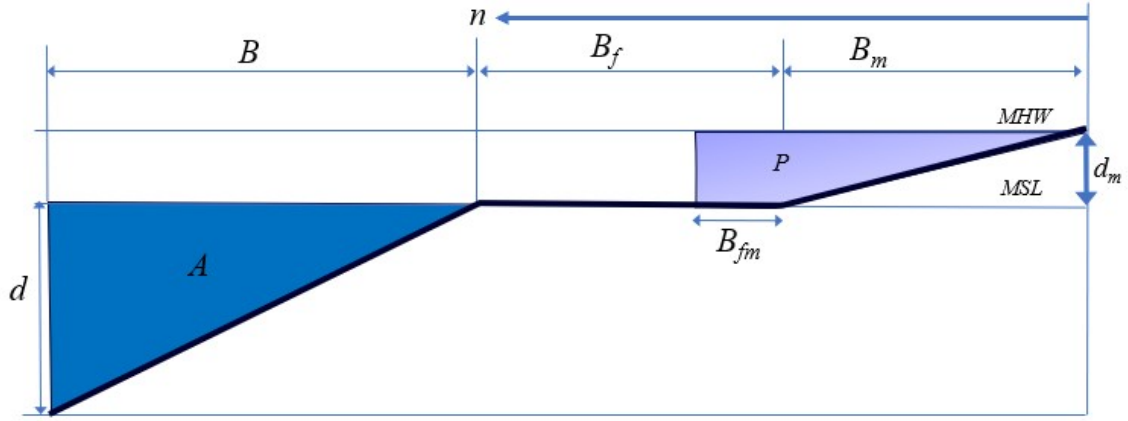
FIGURE 4: Cross-shore profile ShorelineM (personal communication with D. Roelvink, 6 December, 2023)

If the coast is accreting, the cross-shore profile looks different, which is presented in figure 5. The areas that have been accreted are shown in green, and the original profile is shown by the dashed line. The position of the cross-shore coordinate n moves seaward over a distance Δn.
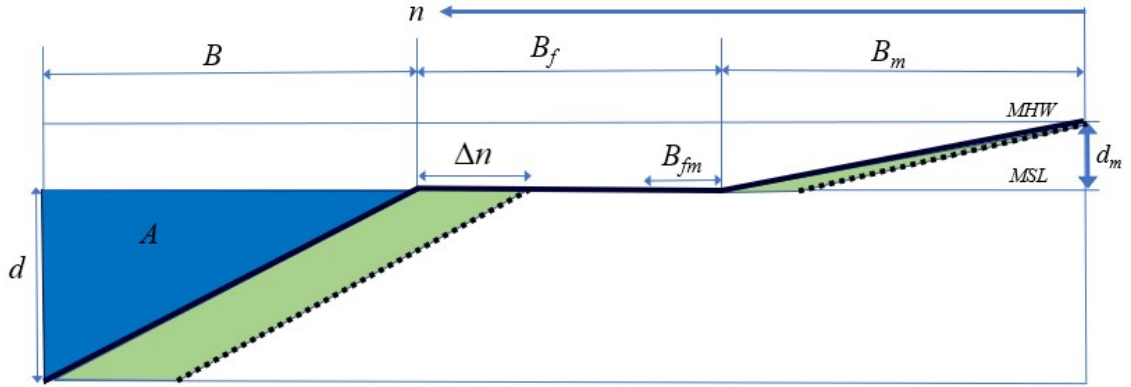
FIGURE 5: Cross-shore profile of ShorelineM that has accreted over a distance Δn. The green areas are the areas that accreted, the dashed line is the original profile.

2.1.1 Model equations

The principles of ShorelineS are used as a basis for ShorelineM, i.e. the position of the shoreline is determined by ShorelineS, which is then used as the basis for ShorelineM. To represent the situation at muddy coasts, Eq.(1) is formulated. In this equation, the change of the cross-shore coordinate over time ($\partial n/\partial t$) is determined by the gradient of the longshore sediment transport (Q_s) (which is determined in Eq.(5)) over the longshore distance s, the relative sea-level rise ($RSLR$), sediment sources (q_{riv}) and sediment sinks (q_m). The longshore gradient, the SLR, the sources and then sinks are all divided by the active profile height (d), see figure 4.

$$\frac{\partial n}{\partial t} = -\frac{1}{d}\frac{\partial Q_s}{\partial s} - \frac{B}{d}RSLR + \frac{1}{d}q_{riv} - \frac{1}{d}q_m \tag{1}$$

The model incorporates sediment sources (e.g., rivers) and sinks (e.g., mangrove forests),

which represent the situation at muddy coasts. In ShorelineM, the evolution of the morphology is determined based on the volume of sediment/mud that is trapped in the mangroves. The relevant processes and essential equations that are used in the model are described below. How these equations are solved in the model and how the equations influence the development of the mud-mangrove areas is described in Appendix A.2.

In ShorelineM, wind-driven currents are the main driver of mud transport and additional forces are caused by waves. The main hydrodynamic equation for the model is the longshore momentum equation, which is averaged over the nearshore cross-sectional area A, see Eq.(2) (Roelvink, 2023):

$$\frac{\partial Av}{\partial t} = \frac{\partial Q}{\partial t} = A\frac{\tau_{w,s} + F_{w,s} - \bar{\tau}_{m.s}}{\rho_w h} = \frac{A(\rho_a C_d u_{10}^2 \sin(\phi_c - \phi_{wind}) + F_{w,s}) - \rho_w c_f u_{rms}Q}{\rho_w h} \tag{2}$$

Where v is the longshore velocity, Q is the longshore discharge, $\tau_{w,s}$ is the wind shear stress, $F_{w,s}$ is the wave forcing, $\bar{\tau}_{m,s}$ is the longshore mean bed shear stress, ρ_w is the density of water, h is the water depth in the foreshore area, ρ_a the density of the atmosphere, C_d the wind drag coefficient, u_{10} the wind velocity at 10 meters high, ϕ_c is the orientation of the shore normal with respect to North, ϕ_{wind} is the angle of incidence of waves with respect to North, c_f the flow drag coefficient and u_{rms} the root-mean square orbital velocity. The wave forcing $F_{w,s}$ is computed according to Eq.(3):

$$F_{w,s} = \frac{1}{32}\rho g H s_{tdp}^2 \sin(2(\phi_c - \phi_w)/B \tag{3}$$

Where g is the gravitational acceleration, $H_{s,tdp}$ is the significant wave height at the toe of the dynamic profile and B is the width of the nearshore zone as already defined in figure 4.

By assuming quasi-stationary conditions, the longshore discharge of water Q can be determined from Eq.(2) by assuming $\partial Q/\partial t = 0$, effectively balancing the long shore wind shear stress and wave forcing with the mean bed shear stress:

$$Q = A\frac{\rho_a C_d u_{10}^2 \sin(\phi_c - \phi_{wind}) + F_{w,s}}{\rho c_f u_{rms}} \tag{4}$$

This momentum balance is visualized in figure 6.
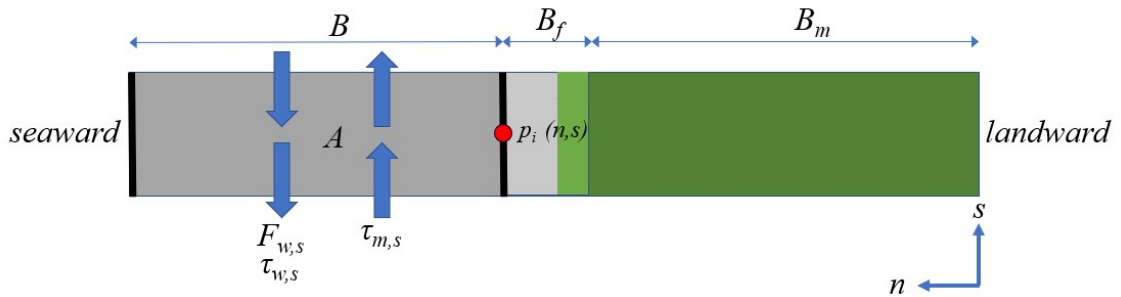
FIGURE 6: Momentum balance ShorelineM, where the wave forcing ($F_{w,s}$) and wind shear stress ($\tau_{w,s}$) are balanced in longshore direction with the bed shear stress ($\tau_{m,s}$) over the nearshore area A (width B) for point p_i.

The longshore discharge from Eq.(4) can be used to determine the nearshore-averaged longshore advection of mud, see Eq.(5). In this equation, the longshore advection of mud results from sediment erosion, deposition and the sediment sources and sinks:

$$\frac{\partial Q_s}{\partial s} = \frac{\partial Q\bar{c}}{\partial s} = \begin{cases} B\left(M\frac{\tau - \tau_{cr}}{\tau_{cr}} - w_s\bar{c}\right) + q_{riv} - q_m \text{ for } \tau \geq \tau_{cr} \\ -Bw_s\bar{c} + q_{riv} - q_m \text{ for } \tau < \tau_{cr} \end{cases} \tag{5}$$

Where $\bar{c}$ is the nearshore averaged sediment concentration, B the width of the nearshore zone, M the erosion factor, τ the shear stress, τ_{cr} the critical shear stress for erosion, w_s the fall velocity, q_{riv} the sediment source induced by the river and q_m the sediment sink which defines the flux of sediment towards the mangroves.

Sediment in ShorelineM is entrained if the shear stress is higher than the critical shear stress ($\tau > \tau_{cr}$), where in ShorelineM τ is defined according to Eq.6:

$$\tau = c_f \rho_w max(v, u_{rms})^2 \tag{6}$$

Where c_f is the flow drag coefficient, ρ_w is the density of water, v is the longshore velocity between two cells and u_{rms} is the root-mean square orbital velocity.

Using the numerical solution scheme from appendix A.2, with the tridiagonal system, the suspended sediment concentration $\bar{c}$ is determined, based on the longshore current, erosion and settling of sediment, river input and sediment fluxes towards mangroves. Multiplying the nearshore averaged sediment concentration $\bar{c}$ with the longshore current Q results in the total longshore sediment current, shown in Eq.(7):

$$Q_s = Q\bar{c} \tag{7}$$

2.1.2 Representation of mangroves in the model

The above presented model equations are used as the basis for the development of mangroves in the model. For the implementation of the mangroves, first the tidal prism P is calculated by the volume of water that enters the mangroves during high tide, as expressed in Eq.(8).

$$P = \left(\frac{1}{2}B_m + B_{fm}\right)d_m \tag{8}$$

The tidal prism is defined by the width of the mangroves (B_m), the width of the colonizing zone of the mangroves (B_{fm}) and the difference in water level between high tide (MHW) and mean sea level (MSL), which is also defined as d_m. With the tidal prism, the sediment flux into the mangroves q_m is then presented by Eq.(9).

$$q_m = 700\frac{\bar{c}P}{\rho_s}max\left(min\left(\frac{B_f - B_{f,crit}}{B_{f,crit}}, 1\right), 0\right) \tag{9}$$

Where 700 is the number of tides per year, $\bar{c}$ the suspended sediment concentration defined with the tridiagonal system presented in appendix A.2, P is the tidal prism, ρ_s is the density of the sediment, B_f is the width of the mudflat and $B_{f,crit}$ is the critical width of the mudflat.

To compute the development of the mangrove- and mudflat area over time, multiple equations are defined which are presented below. First, the development of the cross-shore

coordinate n over time is presented in Eq.(10). The first equation can be used when a mudflat is present in the calculations ($B_f > 0$), then the mangrove area and cross-shore coordinate move separately. If no mudflat is present, the second or third equation has to be used. Then the mangrove area and the cross-shore coordinate move together, depending on the width of the colonizing mangrove area (B_{fm}).

$$\frac{\partial n}{\partial t} = \begin{cases} \dfrac{-\frac{\partial Q_s}{\partial s} - q_m + q_{riv}}{d} & \text{for } B_f > 0 \\[2ex] \dfrac{-\frac{\partial Q_s}{\partial s} + q_{riv}}{d} & \text{for } B_f = 0 \wedge B_{fm} > 0 \\[2ex] \dfrac{-\frac{\partial Q_s}{\partial s}}{d + 0.5 d_m} & \text{for } B_f = 0 \wedge B_{fm} = 0 \end{cases} \tag{10}$$

In Eq.(10) the development of the cross-shore coordinate depends on the longshore gradient of the sediment transport ($\frac{\partial Q_s}{\partial s}$), the sediment flux into the mangroves (q_m), the sediment input from rivers (q_{riv}), the active profile height d and the tidal amplitude d_m.

The development of the mangrove width B_m over time is presented in Eq.(11). Again, the first equation can be used when a mudflat is present in the calculations ($B_f > 0$), then the mangrove area and cross-shore coordinate move separately. If no mudflat is present, the second or third equation has to be used:

$$\frac{\partial B_m}{\partial t} = \begin{cases} \dfrac{2 q_m}{d_m} & \text{for } B_f > 0 \\[2ex] 0 & \text{for } B_f = 0 \wedge B_{fm} > 0 \\[2ex] \dfrac{\partial n}{\partial t} & \text{for } B_f = 0 \wedge B_{fm} = 0 \end{cases} \tag{11}$$

In Eq.(11) the development of the mangrove width depends on the sediment flux into the mangroves (q_m) and the tidal amplitude (d_m). With the development of the cross-shore coordinate and mangrove width, the development of the mudflat width B_f is determined, which is presented in Eq.(12) . If there is no mudflat, there will be no development of the mudflat width:

$$\frac{\partial B_f}{\partial t} = \begin{cases} \dfrac{\partial n}{\partial t} - \dfrac{\partial B_m}{\partial t} & \text{for } B_f > 0 \\[2ex] 0 & \text{for } B_f = 0 \wedge B_{fm} > 0 \\[2ex] 0 & \text{for } B_f = 0 \wedge B_{fm} = 0 \end{cases} \tag{12}$$

The development of the colonizing mangrove width B_{fm} is expressed in Eq.(13):

$$\frac{\partial B_{fm}}{\partial t} = \begin{cases} \varsigma \left(B_f - B_{fm} \right) & \text{for } B_f > 0 \\[2ex] \dfrac{\partial n}{\partial t} & \text{for } B_f = 0 \wedge B_{fm} > 0 \end{cases} \tag{13}$$

Where ς is a factor that determines how fast the colonizing mangrove area extends over the mudflat area (with values between 0 and 1). If its value is 0, there will not be development of the colonizing mangrove width. If its value is 1, the development of the colonizing mangrove width will extend towards the widest point of the mudflat.

Visualization of model simulations

After a simulation, the different mud-mangrove zones have developed towards a certain width. In figure 7, an overview of these different zones (B_m, B_{fm} and B_f) is visualized, where the original coastline is indicated with the red line, and where the simulated coastline is indicated with the black line. For plotting the results, the horizontal axis shows the Easting and the vertical axis shows the Northing.
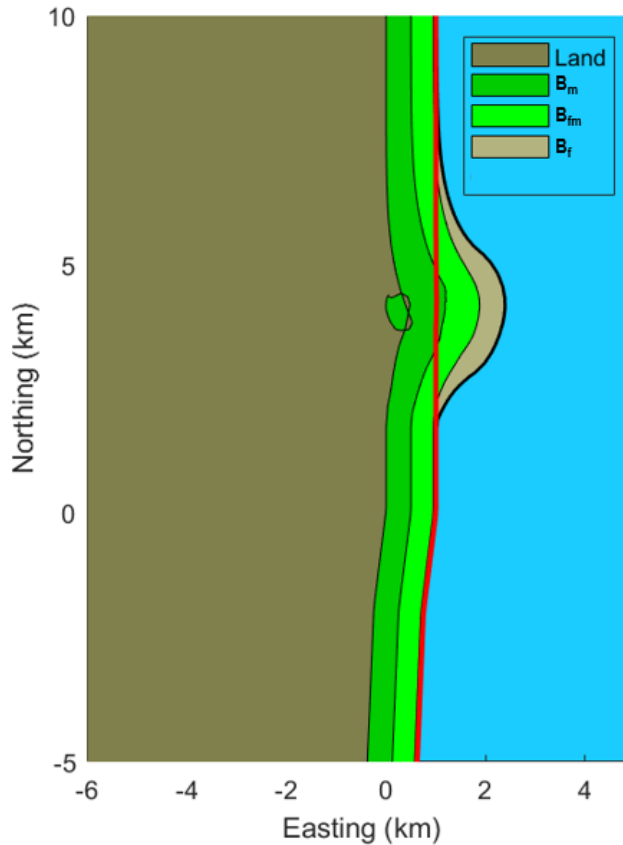
FIGURE 7: Top view of representation of vegetation, with the mangrove area (B_m), the colonizing mangrove area (B_{fm}), the mudflat area (B_f) and the onshore land. The original coastline is visualized in red, and the updated coastline in black. The sea/ ocean is visualized in blue.

2.1.3 Boundary conditions

The model is set-up with boundary conditions for the coastline orientation and the sediment transport gradient. In the initial set-up of the model, both the coastline orientation and sediment transport gradient are supplemented with homogeneous 'Neumann' boundary conditions at the boundaries of the model domain. By applying these conditions to the model, there is a fixed coastline position at both ends of the model. An example of this fixed coastline is presented for an accreting coast in figure 8. In this figure the coastline is fixed at two points; N = 10 km, E = 1 km and N = 0 km, E = 1 km. The coastline is extending at the Northern part of the model, but is fixed to the original boundary of the model and therefore ends at that original boundary:
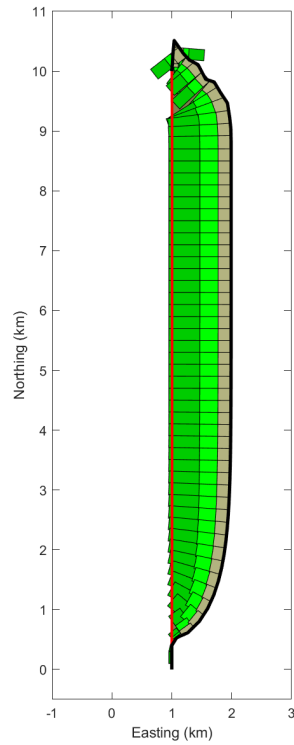
FIGURE 8: Visualization of a coastline orientation with fixed ends at the boundaries of the model. The original coastline is visualized by the red line, the simulated coastline after 20 years is visualized by the black line. The original coastline starts at N = 10 km, E = 1 km and ends at N = 0 km, E = 1 km. The landward side is on the left hand of the red line, whereas the sea/ocean is on the right hand of the red line.

2.1.4 Overview of physical processes

An overview of the relevant processes of ShorelineM is shown in figure 9.
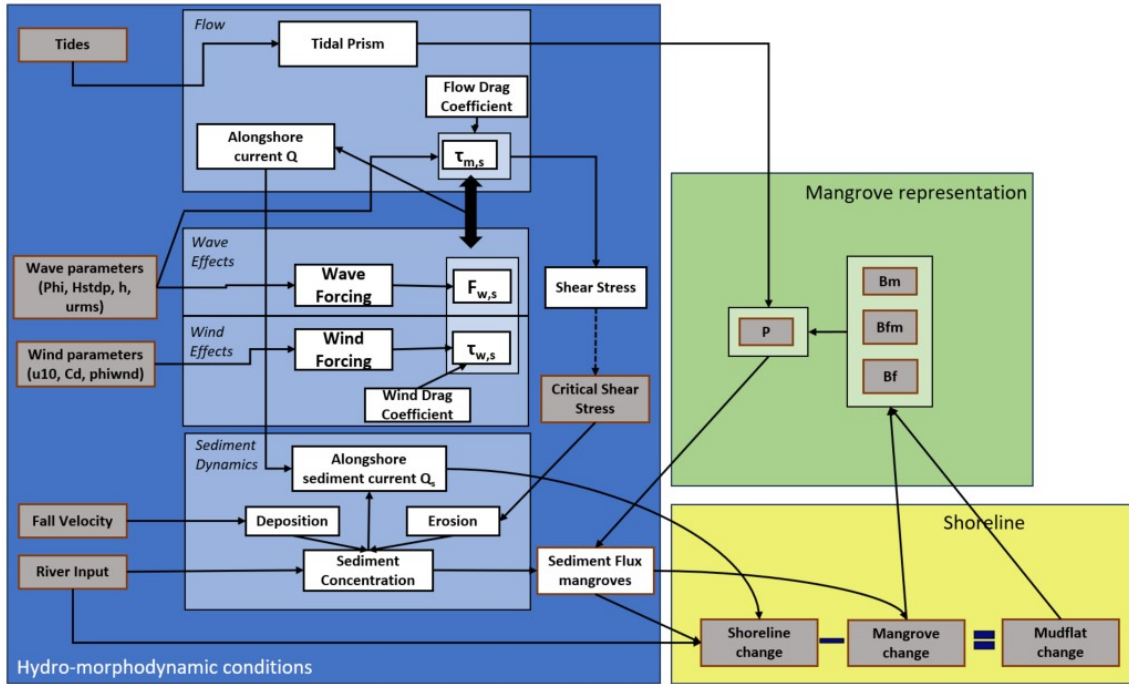
FIGURE 9: Overview of the different processes in ShorelineM. The shoreline- and mangrove change are influenced by the river input, the sediment flux into the mangroves and the alongshore sediment current.

2.2 MFlat

MFlat is a process-based, morphodynamic cross-shore model designed to investigate wave-induced morphodynamics on intertidal mudflats and mangroves (van der Wegen et al., 2019). It is an open-source Matlab code that comprehensively describes both cross-shore and alongshore tidal hydrodynamics, including a stationary wave model, on a high resolution grid, with a small time step (the numerical scheme allows spatial steps of 10 m and a time step of 5 s) (van der Wegen et al., 2019). A visualization of the grid that is used in MFlat is shown in figure 10. The length of the cross-shore domain is indicated as x, which starts at the seaward boundary at $x = 0$m, and ends at the landward boundary at a predefined distance L ($x = L$ m).
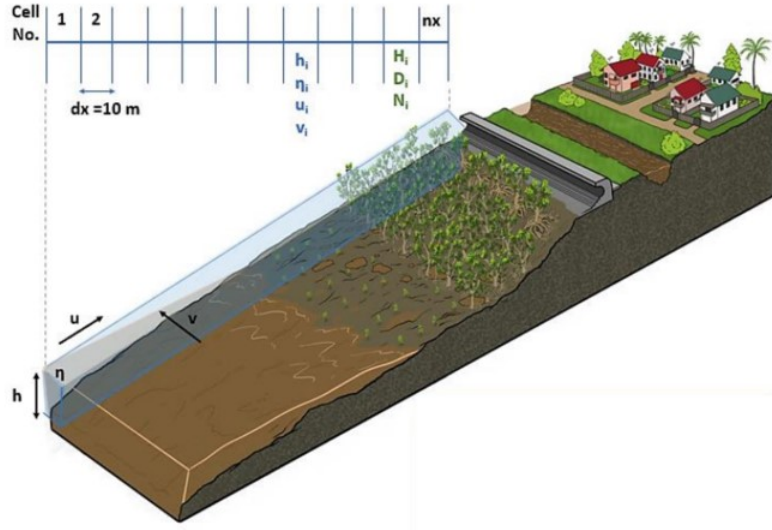
FIGURE 10: Conceptualization of the MFlat grid with a high resolution of 10 m. Where h_i is the water depth at cell i, η_i is the water level at cell i, u_i is the cross-shore velocity at cell i, v_i is the alongshore velocity at cell i, H_i is the mangrove height at cell i, D_i is the mangrove diameter at cell i and N_i is the number of mangrove plants at cell i (Best et al., 2024).

MFlat simulates dynamics that converge to an equilibrium profile based on the given conditions (Best et al., 2024). Normally, the dynamic equilibrium of mangroves is reached after 50-70 years, depending on the initial conditions (Fromard et al., 1998). In the model, this equilibrium can be reached earlier by increasing the growth parameter G of the mangroves (Best et al., 2024).

2.2.1 Hydrodynamics

In MFlat, hydrodynamic processes as tides and waves are represented by a simplification of the shallow water equations (van der Wegen et al., 2019). The cross-shore velocity is calculated with mass-balance equation instead of the momentum equation. In this equation, the inertia and friction effects are neglected.

$$(hu)_i = \frac{dh_i}{dt} X_i \leftrightarrow u_i = \frac{dh_i}{dt} \frac{X_i}{h_i} \tag{14}$$

Where h_i is the water depth at cell i, u_i is the cross-shore velocity at cell i and X_i is the distance from cell i to the land boundary.

In this study, the alongshore current is switched off, as this would affect the way MFlat simulates the dynamics that result in an equilibrium profile. The alongshore velocities are an order of magnitude larger than the cross-shore velocities (van der Wegen et al., 2019). The generation of waves through wind is also switched off in this study, as the cross-shore model domain is too short to have impact on it and it further increases the wave heights, which is not necessary for determining the cross-shore dynamics of mangrove forests.

During a tidal cycle, the water levels on the mudflats increase and the cross-shore velocities at these flats increase too. Before the maximum water level is reached, the cross-shore velocities decrease. At the highest water level, the velocity is zero (slack tide). Afterwards, the water level decreases and velocities increase again. Before the minimum

water level is reached, the cross-shore velocities decrease until the lowest water level. This process is visualized in figure 11a. This visualization of the tidal velocity is plotted for the situation which is shown in figure 11b. In the model there is tidal symmetry, as ebb and flood values are equal. The tidal amplitude that is used in this situation is a constant value. By the hydrodynamics in the model, a symmetric tidal signal is produced.
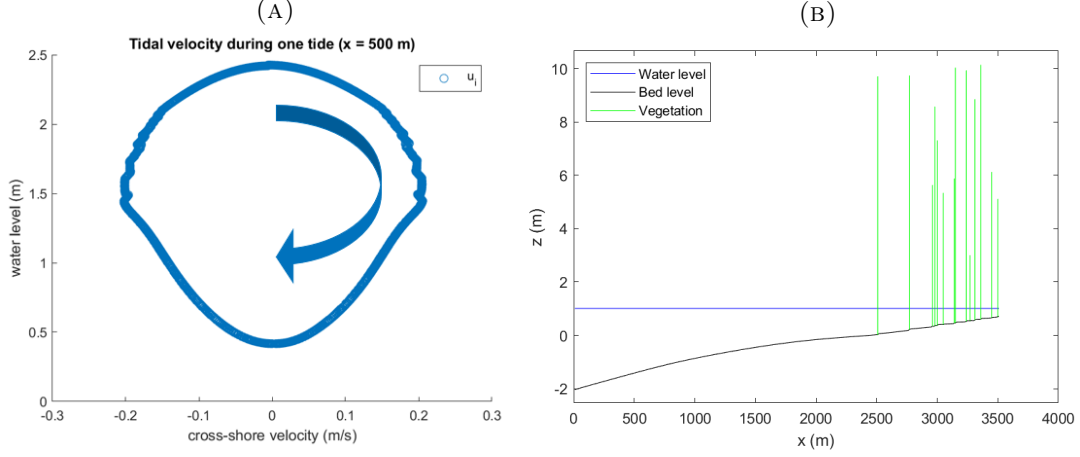
FIGURE 11: Cross-shore velocities during one tidal cycle. (A) Cross-shore velocity during a tidal cycle in MFlat. (B) Situation where the cross-shore velocity is plotted, at x = 500 m.

2.2.2 Sediment dynamics

In MFlat, the sediment transport fields are determined by the Partheniades-Krone formulations (Krone, 1962; Partheniades, 1965), which focuses on fine cohesive sediments. These formulations are made for erosion and deposition. The erosion term ero is presented in Eq.(15):

$$ero = M\frac{\tau - \tau_{cr}}{\tau_{cr}} \tag{15}$$

Where M is the erosion factor, a calibration parameter that determines how much sediment is entrained from the bed, τ is the total shear stress and τ_{cr} is the critical shear stress. The total shear stress consists of the wave- and current induced shear stress (τ_w and τ_c). If the actual total shear stress is higher than the critical shear stress τ_{cr}, sediment is entrained from the bed. This fraction of the shear stress is multiplied with the erosion factor M. The deposition term $depo$ is presented in Eq.(16):

$$depo = w_s c \tag{16}$$

Where w_s is the fall velocity and c is the sediment concentration. This sediment concentration is influenced by the amount of deposited- and eroded sediment and the boundary sediment concentration c_{bcs} that is an input parameter at the seaward boundary of the model. This parameter determines how much sediment enters the model at the boundary.

An advection-diffusion equation describes the transport of entrained sediment in cross-shore direction, which is presented in Eq.(17). This cross-shore transport of sediment results in erosion and deposition of sediment at the bed:

$$\frac{\partial hc}{\partial t} + \frac{\partial uhc}{\partial x} - D\frac{\partial h\frac{\partial c}{\partial x}}{\partial x} = ero - depo \tag{17}$$

Where c is the concentration [kg/m^3 or g/l], D is the diffusion coefficient [m^2/s], and *ero* and *depo* are the erosion and deposition terms.

2.2.3 Morphodynamics

The change in bed level over time is computed by the local sediment transport gradient (depending on advection and diffusion) together with erosion and deposition terms, which is multiplied by a morphological factor (van der Wegen et al., 2019). The morphological factor accelerates the simulated morphological development, as morphodynamic processes have a longer time scale than the hydrodynamic processes (Ntriankos, 2021). The bed level change is expressed in an equation and shown in Eq.(18) (van der Wegen et al., 2019).

$$\frac{\partial z}{\partial t} = M_f \left[\frac{\partial uhc}{\partial x} - D \frac{\partial h \frac{\partial c}{\partial x}}{\partial x} + \frac{(\text{depo-ero})}{\rho_b} \right] \tag{18}$$

Where z is the bed level, M_f is the morphological factor, u is the cross-shore velocity, h is the water depth, c is the concentration, D is the diffusion coefficient, ρ_b the bulk density of sediment and *depo* and *ero* are the deposition and erosion terms, as explained above. Following the accumulation of organic matter, the bed level can further increase. The equation of this organic accumulation is shown in Appendix A.3.

2.2.4 Vegetation dynamics

The vegetation dynamics are based on the windows of opportunity concept, which was included in a second version of MFlat, described by Alexandre Legay (Legay, 2020). In this version of MFlat, the colonization of *Avicennia germinans* is simulated across the domain. This species of mangrove has a root system with pneumatophores, which is included in the parameters in the model. The model divides mangrove development in four different stages; initial establishment of vegetation, establishment of new vegetation every year, growth of vegetation and death of vegetation.

Vegetation is initialized in the model only if the hydroperiod P_t (fraction of time that a certain bed level is below the water level) is smaller than 0.5. If the bed level is above the water level for some period, there is a probability that vegetation starts to grow at a cell in the model. This probability is location-specific and can be changed to a desired value. Besides this probability, there is also a probability for new vegetation to appear during the simulation, which is also location-specific. The growth of vegetation depends on multiple conditions as competition, inundation and salinity. In the model it is described by a sigmoid function, which uses a upper limit of the tree size (with D_{max} and H_{max}) (Best et al., 2024). The growth of vegetation is described by Eq.(19);

$$\frac{dD}{dt} = GD \frac{\left(1 - \frac{DH}{D_{max}H_{max}}\right)IC}{247 + 3b_2 D - 4b_3 D^2} \tag{19}$$

Where G is the mangrove growth parameter, D is the mangrove diameter, H is the mangrove height, D_{max} the maximum mangrove diameter, H_{max} the maximum mangrove height, I the inundation stress parameter (related to P_t), C the competition stress parameter and b_2 and b_3 dimensionless growth parameters.

The three different stages of the vegetation highly depend on the product of IC in Eq.(19). If the product of the inundation stress I and the competition stress C is lower than 0.5, the mangroves do not grow anymore (Ntriankos, 2021) and some trees eventually

die. This then decreases the competition, which increases the value of C again, as with a higher value for C mangroves grow without competition stress. The inundation stress depends on the hydroperiod P_t. If a tree is submerged under water for more than 50 % of the time, the inundation stress factor is 0, and the plants do not grow.

The influence that the vegetation has on the physical processes (i.e. hydrodynamics and sediment dynamics) is described in Appendix A.3.

2.2.5 Overview of processes

The hydro-, sediment- and vegetation dynamics interact, which is schematized in figure 12. Here it can be seen that the vegetation dynamics have influence on the sediment- and morphodynamics and the waves. Whereas the vegetation itself is mostly influenced by erosion/deposition and the tides. The sediment dynamics are mostly influenced by the hydrodynamics (tides and waves), the bathymetry and the calibration parameters (critical shear stress, boundary concentration and settling velocity).
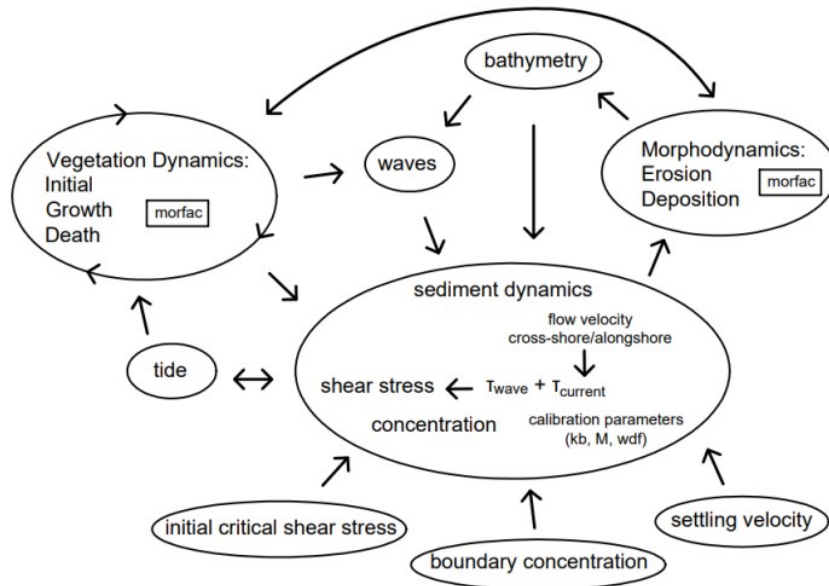
FIGURE 12: Overview of the processes and interactions in MFlat (Ntriankos, 2021).

2.3 Coupling of MFlat and ShorelineM

Both models act on different timescales and include different processes. Real-time coupling of these models (1-on-1), where parameters are transferred after every time step, is increasing the simulation time of ShorelineM too much. This short simulation time is one of the advantages of ShorelineM, and it is therefore desired to preserve these short simulation times. Therefore, the development towards the equilibrium situation of MFlat (after 40 years) is used to provide ShorelineM with information of the cross-shore morphodynamics in MFlat. This coupled model will be applied to an idealized testcase in Guyana, this testcase is explained in chapter 2.3.1. How both models (ShorelineM and MFlat) are set-up is presented in chapter 2.3.2 and chapter 2.3.3. How the information of the cross-shore morphodynamics is produced is elaborated in chapter 2.3.4. A schematization of the coupling is presented in chapter 2.3.5.

2.3.1 Idealized testcase at Guyana

The mangrove coastline of Guyana is under significant pressure from both landward and seaward sides. Land use changes, such as converting agricultural land to residential areas, and the removal of mangroves for fisheries and sea defenses, have reduced the capacity of mudbanks to attach to the coast (Best et al., 2022b). Offshore mudbank dynamics also affect sediment delivery to the mangroves, further hindering regeneration. Historically, the mangrove belt covered the entire coastline, but by 2001, there was a 72% reduction in coverage (Best et al., 2022b). To recover the coverage of mangroves along the shoreline and to increase the attenuation capacity for storms, the Guyana Mangrove Restoration Project started in 2011. For this project thousands of mangrove seedlings were planted along the coast (Ntriankos, 2021).

The coupled model will be applied to the coast at Guyana, to assess whether the model results represent the situation in the field. For this comparison, the coast of Guyana is chosen as the mangrove coastline is under significant pressure and therefore a lot of field data has been collected at a site along this coast. This site is the Chateau Margot mangrove - mudflat in Guyana, located 9 kilometers East of the capital Georgetown, see figure 13. Field data of this site was collected between November 2019 and January 2020 by Üwe Best (Best et al., 2022a). While there is a lot of data collected at this location, it is still quite a difficult location as the shoreline and nearshore sub-tidal areas undergo rapid changes because of the cyclic deposition and erosion patterns caused by the mud fluxes of the Amazon river. By these cyclic patterns, the mudbanks along the coast migrate with an average rate of 1 km per year, which means that alternatingly there are periods with a foreshore mudbank and periods without these mudbanks (which is called the interbank phase). These phases have a duration of 20 to 40 years (Best et al., 2024). Because of this cyclicity, the mudflats and mangroves in the models can best be described as a schematized mudflat inspired by Guyana conditions. As the conditions change over time, there is no stable Guyana mudflat. (Best et al., 2022a).

FIGURE 13: Location of idealized testcase at the Guyana coast near Georgetown. The study area is visualized in the blue box in the left figure, whereas the field data that is used is collected in the green box in the right figure. The right figure is the area in the blue box zoomed in (Google Maps, s.d.).

Along the Guyana coast, there are wave-dominated mangrove forests which are influ-

enced by oceanic swells and semi-diurnal tides. At the Chateau Margot location, there is almost no longshore current by the tides, as filling and emptying of the coastal system occurs perpendicular to the coast (Best et al., 2024). Along the Chateua Margot mudflat, wave heights H_s varied from 0 to 0.65 m, with a mean value of 0.18 m. Mean wave periods T_m varied from 0 to 5.5 s, with an average value of 2.0 s.

2.3.2 Set-up ShorelineM for idealized testcase

As mentioned before, the study area that is used for this study is the coast of Guyana, see chapter 2.3.1. This location is also used for the prior calibration of MFlat and field data is collected at this site (Ntriankos, 2021; Best et al., 2022a). With the models, it is only possible to schematize the mudflat based on the conditions at the Guyana coast. However, these conditions vary a lot, as the Guyana coast is very dynamic and the availability of sediment hugely depends on sediment plume from the Amazon (Best et al., 2022a).

For the simulations a significant wave height $H_s = 0.27$ m is used, with a shear stress $\tau = 0.30$ Pa (Best et al., 2022a). The simulation period was set up to 40 years, to correspond the length of the MFlat simulations. Wind (with a velocity $u_{10} = 10$ m/s) and waves approach the coast at an angle $\phi_w = 135$ deg, which is determined based on the available field data (Augustinus, 1978; Best et al., 2022a).

Static sediment condition

The ShorelineM-model with static sediment conditions is built up as shown in figure 14. The model is built up as a 20 km long straight coast, with sediment input by a river q_{riv} at the yellow arrow ($Northing = 4.0km$). The river input $q_{riv} = 5.0 \times 10^6$ m^3/year (Winterwerp et al., 2007), which represents the mud fluxes along the coast. The initial mudflat- and mangrove width is defined as 25 meter, as there has to be a minimum width to start the simulation (Roelvink, 2023).
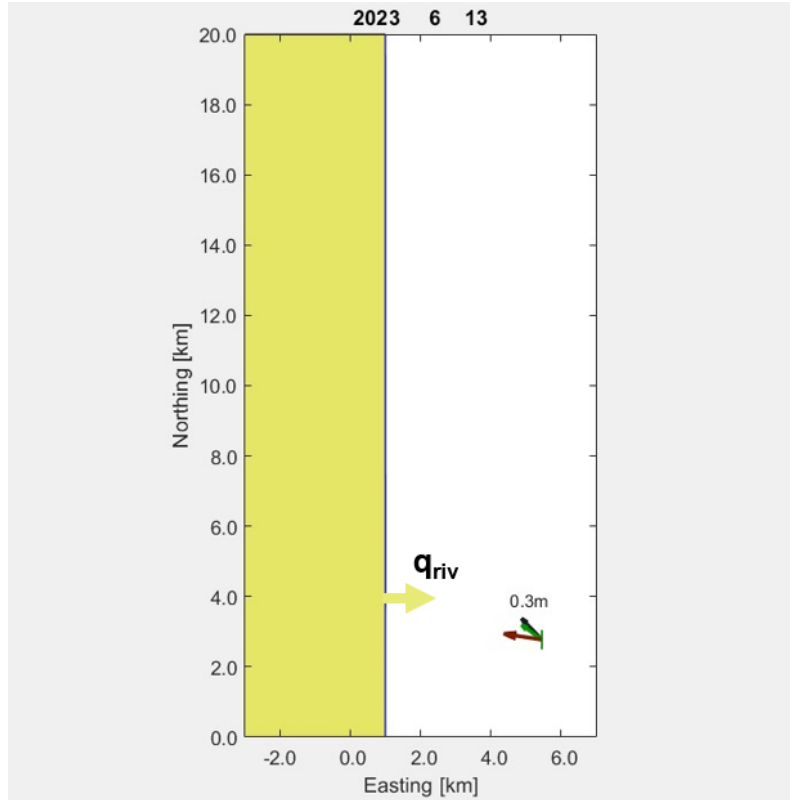
FIGURE 14: Overview of the set-up of the idealized testcase in ShorelineM.

Cyclic sediment condition

As the conditions above do not completely represent the situation at Guyana (with moving mud banks in front of the coast), a set-up with cyclic sediment input is made too. In this situation the location of the river input changes over time, representing the moving mud banks, and starts at N = 4 km. Every half a year the river input moves 2 kilometers Northwards until N = 18 km. After 4 years it then starts again at N = 4 km, which thus creates sediment cycles of 4 years, see figure 15. The river input is the same as in the previous situation, i.e. $q_{riv} = 5.0 \times 10^6$ m^3/year. The direction of wind and waves is also the same as in the previous situation.
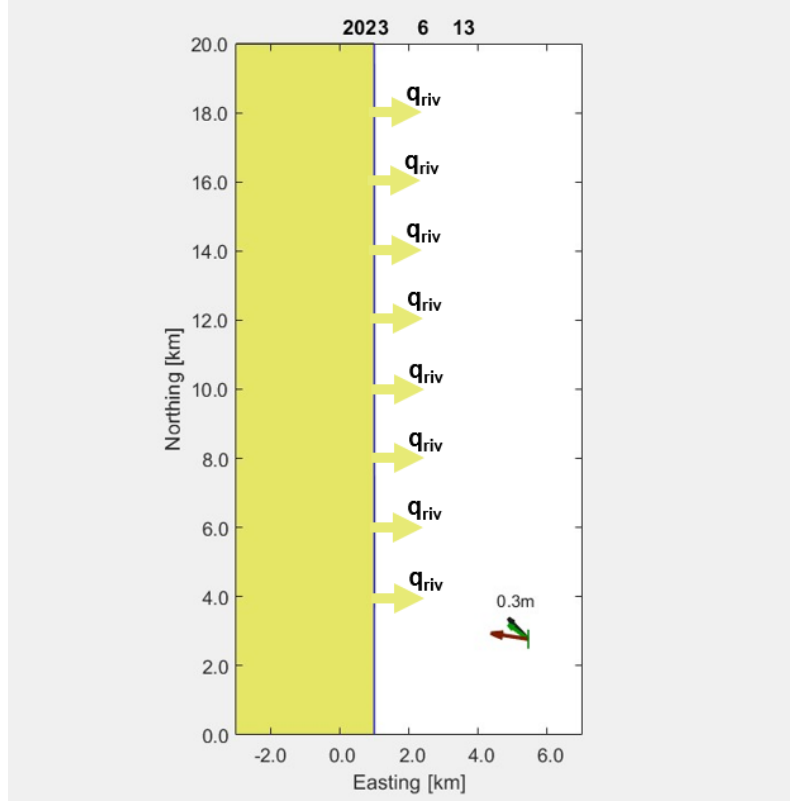
FIGURE 15: Set-up for the cyclic conditions in ShorelineM. Where the input of the river q_{riv} is moving along the coast in Northern direction.

2.3.3 Set-up MFlat for idealized testcase

The initial profile that is used for the simulations has a length $L = 3500$ meter, and a predefined slope $S = 0.001$ m/m. The profile starts at the seaward boundary at a bed level $z = -3.50$ m and ends at the landward boundary at MSL ($z = 0.00$ m). The other parameters that are used in the model are shown in table 2. With this set-up, there will not be mangroves at the beginning of the simulation, which therefore not influences the shear stresses (and the development of the bathymetry) from the beginning. Otherwise, if the initial profile has bed levels above MSL, mangroves may grow there, which decreases the shear stresses and has a positive effect on the accretion of the bed levels around the mangroves.

Parameter	MFlat name	Value
Wave height (H_{rms},m)	HH	0.10 - 0.50
Boundary Sediment concentration (c_{bcs},g/l)	Bcs	0.05 - 0.50
Peak wave period (T_p, s)	Tpp	4.40
Tidal amplitude (d_m, m)	etamp	1.00
Critical shear stress (τ_{cr}, Pa)	taucr	0.30
Erosion factor (M, kg/m^2/s)	MM	0.8×10^{-4}
Fall velocity (w_s, mm/s)	ww	0.30

TABLE 2: Model parameter settings and ranges for obtaining cross-shore dynamics of the Guyana coast (Best et al., 2022b)

The simulations are used to retrieve information of the equilibrium situation (at the end of the simulation, i.e. 40 years) and of the dynamic situation (i.e. the sediment fluxes and sediment trapping). For determining the sediment fluxes, the time-interval of saving the data has to be decreased, as in the default situation, the data is only saved twice during a tidal cycle (at ebb and at flood). To quantify the cross-shore fluxes, the time interval for saving is decreased from every 6 hours to every 10 minutes (without morphological factor). Which means that 36x more steps were saved. Without these smaller steps it would be impossible to precisely determine the cross-shore sediment flux, as at ebb or flood the direction of the cross-shore velocity switches. This velocity is used to determine the flux. The parameters that are saved with this new time-interval are the water depth h, the concentration c, the bed level z and the cross-shore velocity u.

The cross-shore fluxes in MFlat are calculated by computing the suspended sediment flux in cross-shore direction. The flux is calculated by multiplying the concentration, cross-shore velocity and water depth, based on Chen et al. (2018).

$$Q_m = hcu \tag{20}$$

Eq.(20) results in the flux Q_m with a unit of $\frac{\text{kg}}{\text{m}}$/s. Integrating this over time t at a location x results in the sediment flux q_m that has passed that location during a certain time period.

$$q_m = \int_{t1}^{t2} q_m(x,t)dt \tag{21}$$

2.3.4 Library of cross-shore dynamics to obtain in MFlat

To capture the cross-shore morphodynamics of the mangrove forests at the Guyana coast, multiple simulations are executed in MFlat. In MFlat, these simulations will cover a boundary sediment concentration c_{bcs} ranging from 0.05 g/l to 0.50 g/l, and a wave height H_{rms} ranging from 0.10 m to 0.50 m, which can be seen in table 3. This ranges will be used based on field data collected at the Guyana coast and results from MFlat for the Guyana coast (Best et al., 2022b; Ntriankos, 2021). From the simulations, the characteristics at the end of the simulation will be used to create a library of the cross-shore equilibrium for multiple hydrodynamic conditions. The simulations will represent different hydrodynamic situations at the coast of Guyana, which is described in section 2.3.1.

		Boundary sediment concentration c_{bcs} [g/l]				
		0.05 g/l	0.15 g/l	0.20 g/l	0.35 g/l	0.50 g/l
Wave height H_{rms} [m]	0.10 m	✓	✓	✓	✓	✓
	0.15 m	✓	✓	✓	✓	✓
	0.20 m	✓	✓	✓	✓	✓
	0.25 m	✓	✓	✓	✓	✓
	0.30 m	✓	✓	✓	✓	✓
	0.35 m	✓	✓	✓	✓	✓
	0.50 m	×	×	×	×	✓

TABLE 3: Conditions that are used for the different simulations. For the lower boundary sediment concentrations, the bed was already eroded for a wave height $H_{rms} = 0.35$ m. Therefore, only one simulation was made with a wave height $H_{rms} = 0.50$ m.

2.3.5 Schematization of coupling of ShorelineM and MFlat

The information saved in the library is used to inform ShorelineM about the cross-shore development for a certain condition. For every time step ShorelineM models a variable sediment concentration $\bar{c}$ and wave height H_s along the coast. This information from ShorelineM is used to get information about the cross-shore equilibrium from MFlat. The information that is used from the equilibrium situation is the width of the mudflat (B_f), the width of the mangroves (B_m) and the simulation time. An overview of this coupling is shown in figure 16.

With the computational time of MFlat, it takes several days to create such a library. However, after the library is created with enough data, it can represent the cross-shore dynamics for different conditions. Using this information in ShorelineM does not increase the computational load of ShorelineM, which is the case if a dynamic coupling is applied.
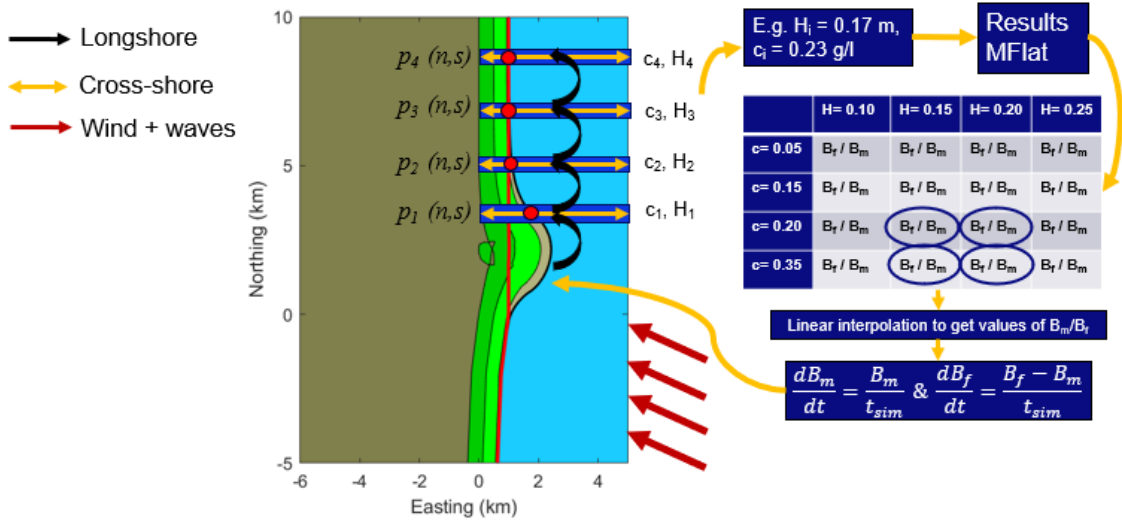
FIGURE 16: Schematized overview of the coupling of both models. With c_i the concentration and H_i the wave height. The modeled concentration at each cell c_i and wave height at each cell H_i from ShorelineM is used to retrieve cross-shore information from MFlat. The development of the mangroves in ShorelineM is then determined by the information from MFlat.

A schematization of where the MFlat-results are implemented in ShorelineM is shown in figure 17. This figure shows the initialization and phases of a ShorelineM simulation, where the basis of ShorelineS is used to initialize the model and where mud transport is introduced in the phase of sediment transport. The library with results of MFlat is introduced in the first phase of ShorelineM. After the tidal prism P, the concentration C and the flux into the mangroves q_m are determined in ShorelineM, the rate of change of the mangrove- and mudflat area is calculated with information from MFlat ($B_{m,lt}$ & $B_{f,lt}$), see Eq.(22).:

$$\frac{dB_m}{dt} = \frac{B_{m,lt}}{t_{sim}} \text{ and } \frac{dB_f}{dt} = \frac{B_{f,lt} - B_{m,lt}}{t_{sim}} \tag{22}$$

Where $B_{m,lt}$ is the width of the mangrove area in MFlat, $B_{f,lt}$ is the width of the mudflat area in MFlat, t_{sim} is the simulation time of the simulations in MFlat in years. The mangrove width $B_{m,lt}$ and mudflat width $B_{f,lt}$ are retrieved from the library with cross-

shore information from MFlat. The rate of change in ShorelineM is multiplied with the time step (dt = 30/365) to calculate the rate of change per month.
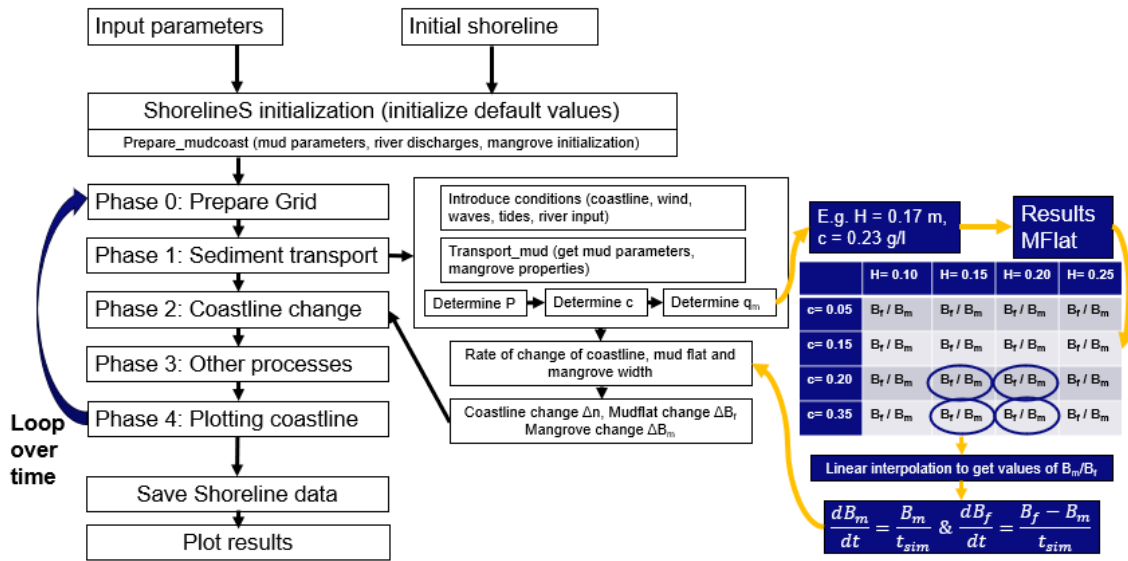
FIGURE 17: Scheme of the different phases of simulation in ShorelineM, which still includes the initialization in ShorelineS. In this scheme, the results of MFlat are included in the computation of the rate of change and are shown by the orange arrows.

3 Formulating model limitations of ShorelineM

The aim of ShorelineM is to model the shoreline development of muddy coasts. In the current version simple assumptions and geometries are used, that have to be proven or that need small improvements for modelling the long-term development of mangrove forests. This chapter shows for some characteristics how realistic the model is and visualizes shortcomings and improvements based on multiple simulations with the model. Possible improvements for these limitations are explained in this chapter and it will be indicated which improvements will be incorporated in the model. Overall, this chapter aims to answer research question RQ1.

3.1 Conservation of cross-shore profile shape

One of the main principles of ShorelineM is the conservation of sediment, which is quantified in Eq.(1) for muddy coasts. This equation describes that all the sediment that enters the model along the whole domain (q_i) is transported along the domain ($\frac{\partial Q_s}{\partial s}$), has influence on the change of the cross-shore coordinate ($\frac{\partial n}{\partial t}$) or the availability of it is reduced by the sea level rise ($RSLR$). In the current version of ShorelineM, SLR was not implemented correctly and therefore switched off. SLR then does not influence the coastline change. Without SLR, the sediment input by rivers in the model is transported along the coast, resulting in a coastline change or a combination of both.

Two simulations with a different sediment input by the river are executed that show how this equation influences the coastline change, see figure 18. All the sediment in this simulation is discharged through the river, and no sediment is entrained from the bed ($\tau < \tau_{cr}$) or supplied at the boundary (no boundary condition for sediment). For the sediment discharged through the river, two different values of sediment input (q_{riv}) were used. In figure 18a a value of 1×10^6 m^3/year is used, whereas the used value in figure 18b was ten times higher and had a value of 1×10^7 m^3/year. The simulation with a ten times higher sediment input resulted in a ten times greater seaward progression of the coastline than the lower sediment input, as can be seen in both figures and in table 4. The area that is measured is the area between the modeled shoreline after 20 years (black line) and the initial shoreline (red line). In this figure, the model domain in Northern direction was from N = -4 km to N = 20 km, in Eastern direction the model domain had no boundaries. The wave height $H_s = 0.20$ m, the critical shear stress $\tau_{cr} = 0.35$ Pa and the fall velocity $w_s = 0.25\times10^{-3}$ m/s.

Simulation	q_{riv} [m^3/year]	Area [km^2]
Low volume	1×10^6	4.69
High volume	1×10^7	44.20

TABLE 4: Calculated area for both simulations in figure 18, where the area in the simulation with a higher volume is ten times higher.
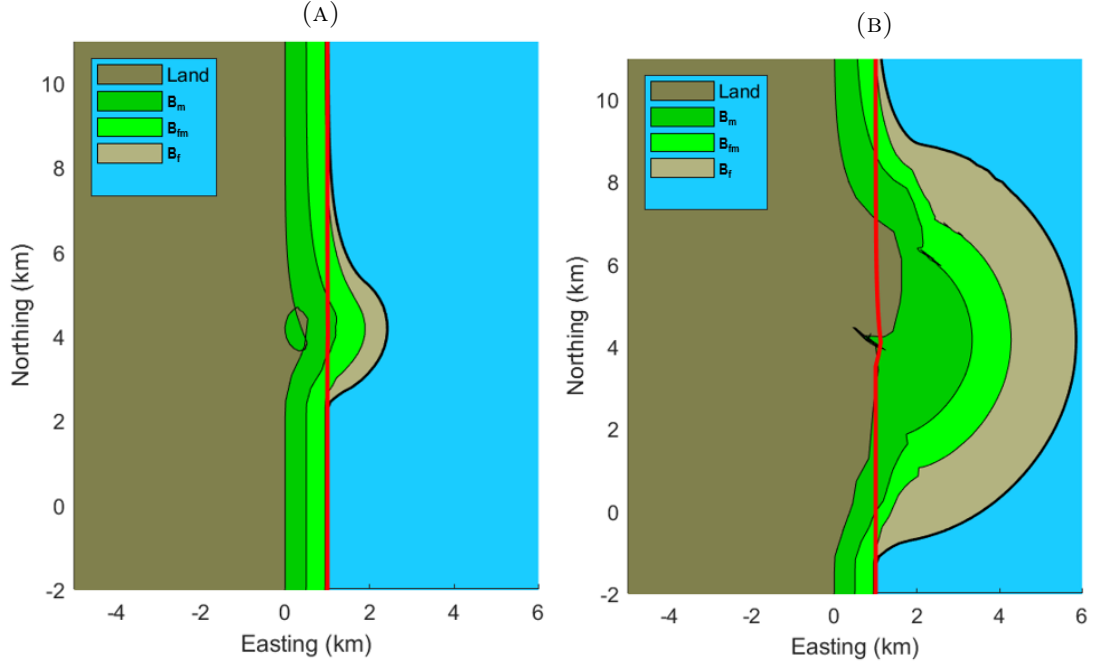
FIGURE 18: Modeled shoreline development after 20 years with differences in sediment input by the river (q_{riv} at Northing = 4 km, Easting = 1 km). (A) Simulation with medium sediment input $q_{riv} = 1 \times 10^6$ m^3/year (B) Simulation with high sediment input $q_{riv} = 1 \times 10^7$ m^3/year.

With this formulation of the coastline change, most of the sediment input results in a seaward movement of the coastline, which provides limited information about the development of mangrove forests. Figure 18 shows the simulated shoreline development and projects a certain mangrove extent based on the tidal prism and the suspended sediment concentration. This does not capture other cross-shore dynamics as a change of the shape of the cross-shore profile and a change of flow characteristics through vegetation (Xie et al., 2022).

In the model, no changes in the shape of the profile are made, which realistically would have happened. If changes of the profile would have been implemented in ShorelineM, sediment would also accrete the profile, which is yet not implemented in Eq.(1). This change of profile also has influence on the tidal prism, which decreases when the profile is accreting.

3.2 Entrainment of sediment

Another characteristic of the model is the way sediment is entrained from the bed, which is explained in Chapter 2. This formulation only captures flow- or current induced shear stresses and not a combination of both. Therefore another possibility for defining the shear stress, is the definition used in MFlat. In MFlat, the total shear stress (τ_{tot}) is determined by a combination of wave-action and current induced shear stresses (van der Wegen et al., 2019):

$$\tau_{tot} = \tau_w + \tau_{cs} \left[1 + 1.2 \left(\frac{\tau_w}{\tau_{cs} + \tau_w} \right)^{3.2} \right] \tag{23}$$

With τ_w the wave shear stress, and τ_{cs} the current shear stress in longshore direction (s), given by:

$$\tau_w = 0.5 \rho_w f_w u_{orb}^2 \ \& \ \tau_{cs} = \rho_w C_d v |v| \tag{24}$$

Where f_w is the wave friction factor [-], u_{orb} is the orbital wave velocity and C_d is the wind drag coefficient.

When the shear stress in ShorelineM is higher than the critical shear stress (e.g. for a value of the critical shear stress τ_{cr} around 0.20 Pa (Ntriankos, 2021)), some sediment is then entrained from the bed. The amount of entrained sediment is then determined by the ratio between the critical and actual shear stress and the erosion factor M, as introduced in Eq.(5) (Roelvink, 2023). The entrained sediment is then averaged in cross-shore direction over the complete nearshore area A for 1 time step (Josten, 2024). Whereas in reality, the suspended sediment concentration is higher at shallower areas of the bare mudflat, as waves and currents have more influence in shallower areas (Chen et al., 2018). This formulation affects the suspended sediment concentration in ShorelineM.

3.3   Representation of tidal prism

Simulations in ShorelineM showed limitations in the assumption of the definition of the tidal prism. Now, the tidal prism is represented as the area between MSL and MHW for the mangrove zone (triangle) and colonizing mangrove zone (rectangle), see figure 4. In fact, the definition of this prism is correct, as it presents the amount of water that enters the mangrove area. However, the cross-shore profile used for this prism deviates from reality and could be improved.

No change of profile shape

Sediment input in the model domain results in a change of the coastline. It increases the width of the three different zones in ShorelineM, whereas the increase of the (colonizing) mangrove zones is initialized by the tidal prism (Eq.(8)). However, an increasing width of these zones results in the same shapes of the zones. The mudflat and colonizing mangrove area are still flat with an increased width. The mangrove area is still a uniform linear slope with an increased width and a gentler slope, as can be seen in figure 19. In this figure, the initial profile has widths of $B_f = 300$ m, $B_m = 250$ m and $B_{fm} = 50$ m. An expanded profile (not based on a certain case) for a situation with an accreting coastline could have widths of $B_f = 2000$ m , $B_m = 1000$ m and $B_{fm} = 500$ m.
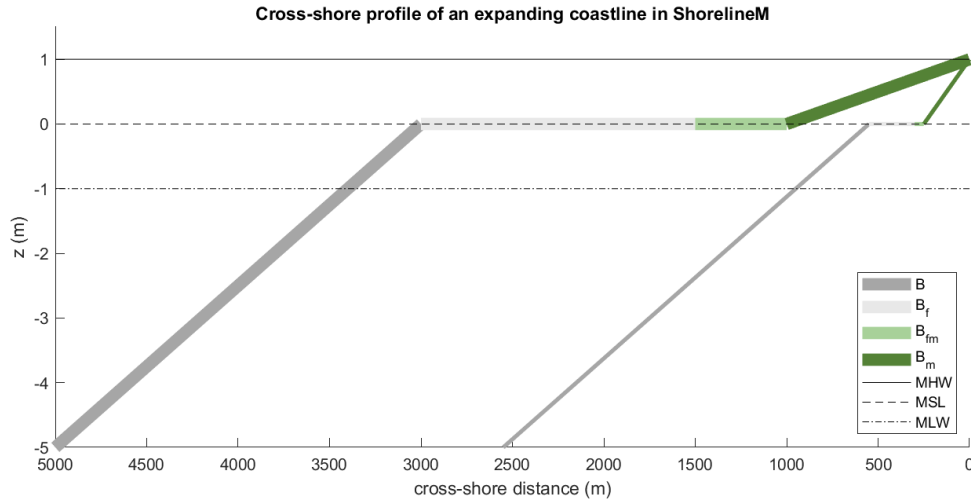
FIGURE 19: Conceptual cross-shore profile of an initial situation (thin colored lines) and expanded situation (thick colored lines) in ShorelineM. The cross-shore distance is measured from the landward side.

In reality a mangrove-mudflat edge is formed which changes the cross-shore profile of mangroves to a convex-up or concave-up profile (Friedrichs, 2011; Xie et al., 2022). An example of a convex-up profile where a mangrove-mudflat edge is formed is presented in figure 20. In this figure, the mangroves are shown in light green, and the mangrove edge is located at a cross-shore distance of around 100 meter, where the bed elevation dropped from 2 m to 1 m above MSL.
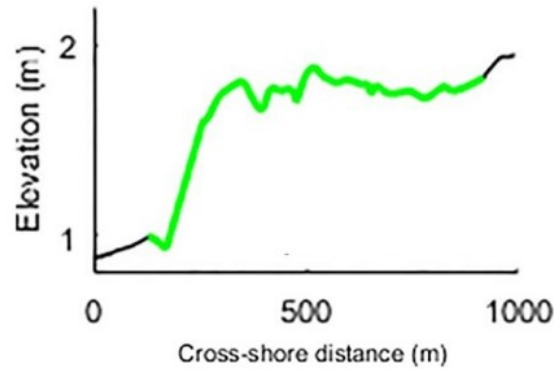
FIGURE 20: Example of convex-up cross-shore profile of a mangrove environment at the Firth of Thames, New Zealand (Bryan et al., 2017).

Changing the cross-shore profile in ShorelineM to the profile presented in figure 20 decreases the size of the tidal prism. With a smaller tidal prism, less water enters the mangrove area, which decreases the sediment input in the area (Horstman et al., 2015).

Increase of tidal prism over time

Due to the representation of the tidal prism as it is visualized in figure 4, the tidal prism keeps increasing over time if the coastline expands too. This can be seen in figures 21a and 21b. However, if there is no SLR (which is the case in the model), the tidal prism decreases over time (in models and in reality) (Xie et al., 2022). This happens as the mangrove area

is accreting towards MSL and less space is available for sediment to enter the mangrove area(Xie et al., 2022).
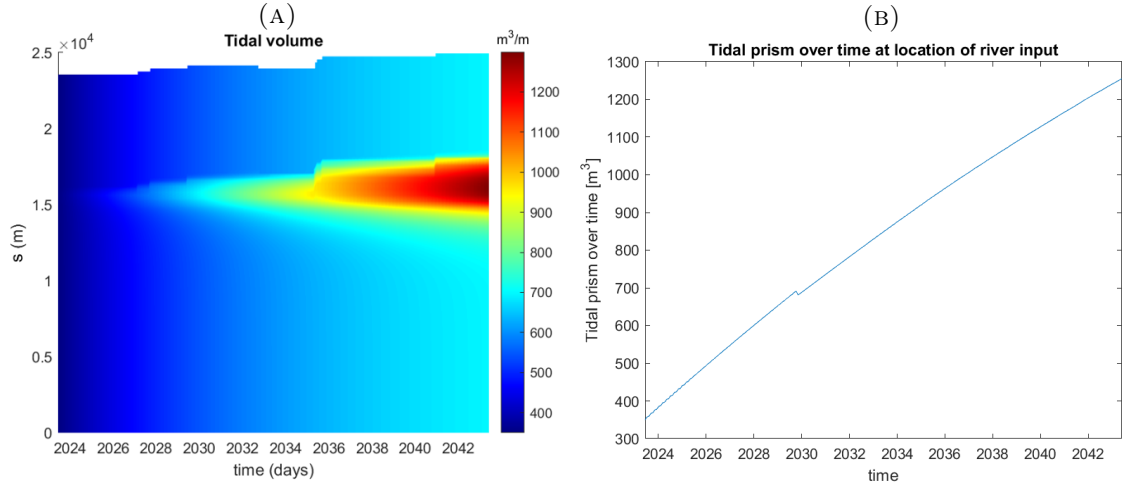
FIGURE 21: Increase of tidal prism over time (A) Development of tidal volume over time and space for the simulation of figure 18a. On the vertical axis the longshore coordinate (s) along the coast is shown, which is along the 24 km long coast used for figure 18, on the horizontal axis the simulation time is shown, which is from 2023 to 2043. (B) Development of the tidal prism at s = 16 km in figure 21a over a period of 20 years.

3.4 Cross-shore fluxes

Besides the conservation and entrainment of sediment, also the transport of sediment in cross-shore direction has its limitations. The cross-shore flux of sediment towards mangroves q_m depends on the tidal prism P, the number of tides during a year and the suspended sediment concentration C. The calculated flux into the mangroves is then used to determine the development of the mangroves, which is shown in Eq.(11) in Chapter 2. This equation can be rewritten such that the flux into the mangroves can be described as the triangle that is visualized in figure 22. This equation is used such that the flux into the mangroves q_m describes the rate of change of the mangrove width, as visualized in figure 22. This triangle shows the deposition across the mangrove area and is thus based on Eq.(9), which is an assumption for the cross-shore fluxes.
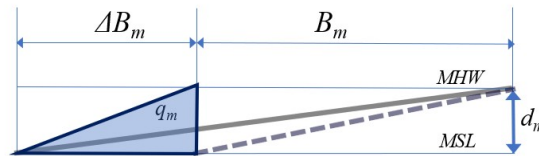
FIGURE 22: Visualization of the sediment flux into the mangroves q_m based on the equation of ShorelineM. The solid line shows the cross-shore profile of the mangrove zone after accreting, the dashed line shows the profile before accreting.

For a preciser quantification of the cross-shore fluxes, it can be based on other software. In this study the cross-shore model MFlat is used, where the cross-shore fluxes are defined with the formulation used by Chen et al. (2018), see Eq.(25). The flux Q_m is based on the

water depth, the suspended sediment concentration and the cross-shore velocity:

$$Q_m = hcu \tag{25}$$

With the cross-shore fluxes used by Chen et al. (2018) and with shear stresses as in chapter 3.2, the deposition and sediment trapping can be determined based on the in- outflow of sediment. This can be used in the coupling between both models.

3.5 Answer to RQ1

The most important limitation in ShorelineM is that the shape of the profile of the mangrove zone does not change, which influences the tidal prism and the cross-shore fluxes. To add these cross-shore dynamics (profile changes and fluxes) MFlat will be used, where the cross-shore dynamics can be simulated in a realistic way. In the next chapter, these cross-shore dynamics from MFlat are elaborated further, to show how it can be implemented in ShorelineM.

4 Analyzing cross-shore dynamics using MFlat

As mentioned before, for improving ShorelineM it is important to explore the cross-shore dynamics of other models. In this study, the cross-shore model that is used for these dynamics is MFlat, and its characteristics are explained in chapter 2. This model simulates dynamics that result in an equilibrium profile in cross-shore direction based on specific conditions (if they are constant over time), so therefore the equilibrium situation is analyzed first. Afterwards, the model results over time are used to determine changes in the cross-shore fluxes and sediment trapping efficiency over time. Overall, this chapter aims to answer research question RQ2.

4.1 Equilibrium situation

For this study, the situation in MFlat after 40 years of simulation is analyzed for the Guyana case (Section 2.3.1). Within these 40 years, the modeled morphology develops towards an equilibrium state, which is fully reached after roughly 60 to 70 years when there are no changes in bathymetry anymore, see figure 23. This situation after 40 years is analyzed for 31 different conditions, as mentioned in section 2.3.4.
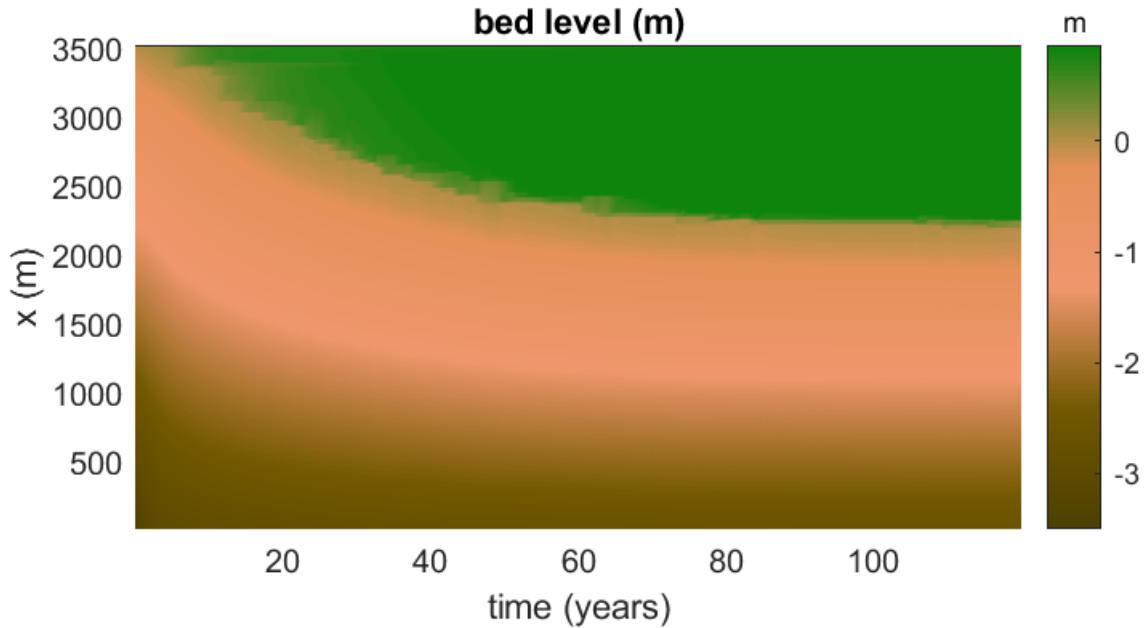
FIGURE 23: Bed level development over time along the model domain, for a simulation with a wave height $H_{rms} = 0.20$ m and a boundary sediment concentration $c_{bcs} = 0.15$ g/l. Around 40 years the model is growing towards an equilibrium, which is reached after roughly 60 to 70 years.

4.1.1 Cross-shore profiles from MFlat

The simulations in the library generate cross-shore profiles based on the different conditions. These profiles visualize the equilibrium situation of muddy coasts for the different conditions which is compared to the cross-shore profile that is used in ShorelineM.

For the situation with a wave height $H_{rms} = 0.20$ m, the cross-shore profiles are presented in figure 24. The initial cross-shore profile is visualized in orange and has a slope of 1/1000. In the figure, it is shown that the condition with the highest sediment supply at

the boundary ($c_{bcs} = 0.50$ g/l, i.e. the yellow line) has the highest lateral expansion of the mangroves, with a width of roughly 2600 meter. The condition with the lowest sediment supply at the boundary ($c_{bcs} = 0.05g/l$, i.e. the dark green line) has almost no lateral expansion of the mangroves, and only has a width of roughly 100 meter.
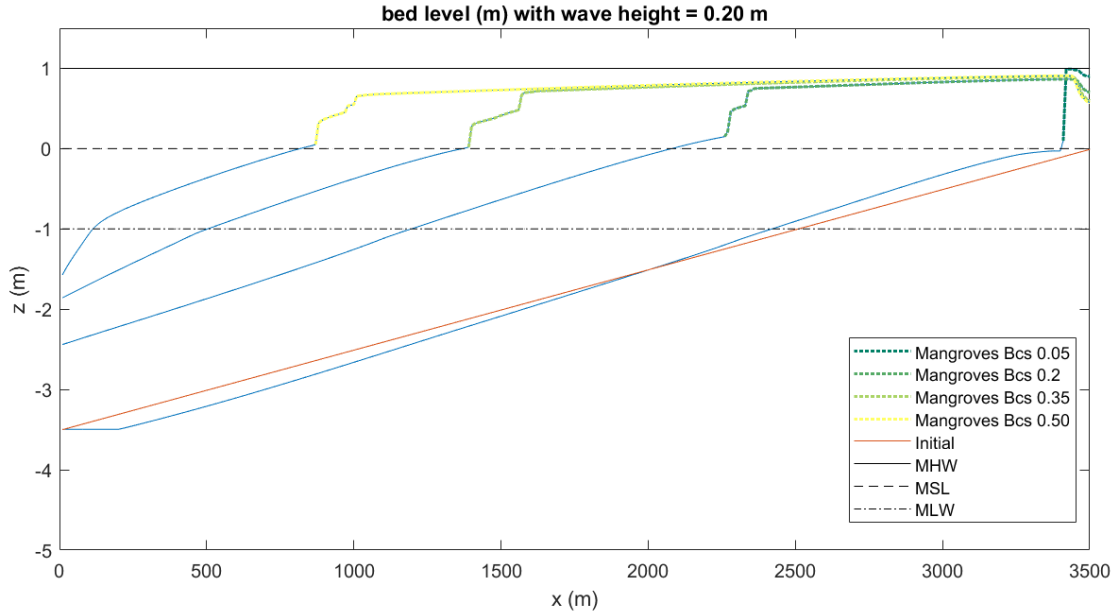
FIGURE 24: Cross-shore profiles of four different simulations in MFlat with a wave height $H_{rms} = 0.20$ m and different boundary sediment concentrations c_{bcs}. The initial profile used for the simulations is shown in orange. For the four simulations, the bed levels below MSL are shown in blue, whereas the bed levels above MSL are indicated with the colors shown in the legend, as at these locations mangroves have grown in the simulation.

Figure 24 shows that the cross-shore profiles of mangrove forests in MFlat are different than the profile that is defined in ShorelineM. In ShorelineM it is defined as a uniform linear slope with a flat colonizing zone in front, see figure 25. However, in MFlat it has a flat zone on the landward side, with a mangrove edge as a transition between the mangroves and the mudflat. The bed levels of the mudflat then gradually decrease, which makes the shape of the mudflat resemble a uniform slope. The difference in these profiles is presented in figure 25.
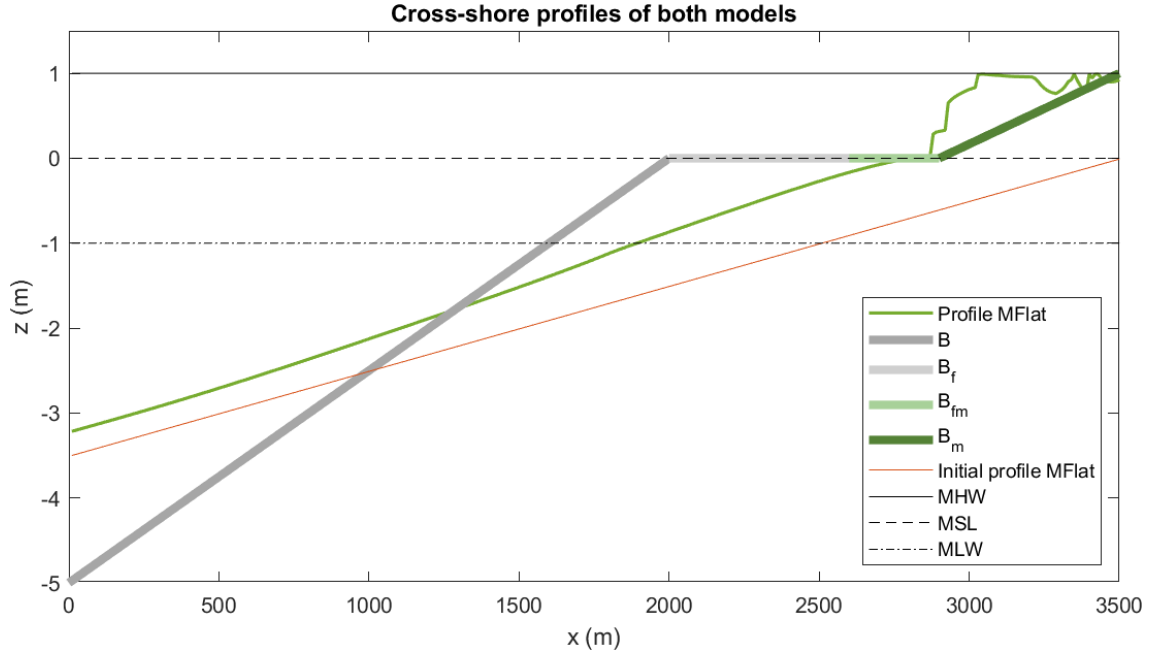
FIGURE 25: Comparison between cross-shore profiles in MFlat and ShorelineM. The MFlat profile is the equilibrium profile after 40 years of simulation for a wave height $H_{rms} = 0.25$ m and a boundary sediment concentration $c_{bcs} = 0.20$ g/l. The profile in ShorelineM is a profile for a fictional case, with a mangrove width $B_m = 600$ m, a colonizing mangrove width $B_{fm} = 300$ m and a mudflat width $B_f = 900$ m.

4.1.2 Effect of wave height and sediment concentration on mangrove characteristics

The equilibrium situation is also used to determine the effect of the wave height and the sediment concentration on different characteristics of the mangrove forests, as the mudflat/mangrove width, the tidal prism and the sediment volume in the mudflat/mangrove area, which is shown below.

Width of the mudflat/ mangrove

From the equilibrium situation of the different simulations, the width of the mangrove area B_m and the mudflat area B_f can be determined. The width of the mangrove area (figure 26a) is determined as the distance between the land boundary ($x = 3500$ m in figure 25) and the point at MSL, which is the lowest possible place for mangroves to grow. The width of the mudflat (figure 26b) is determined as the distance between the land boundary and the point at MLW, as this point is the lowest point that is dry during a tidal cycle. The latter means that the width of the mudflat area is defined as the width of the mangrove area plus the width of the mudflat area in front. Figure 26 shows the width of these areas after the 40 years of simulation for the different conditions (varying wave height and boundary sediment concentration). The width of the colonizing mangrove area B_{fm} is not shown here, as the width of this zone corresponds with the width of the mangrove area in the MFlat simulations.
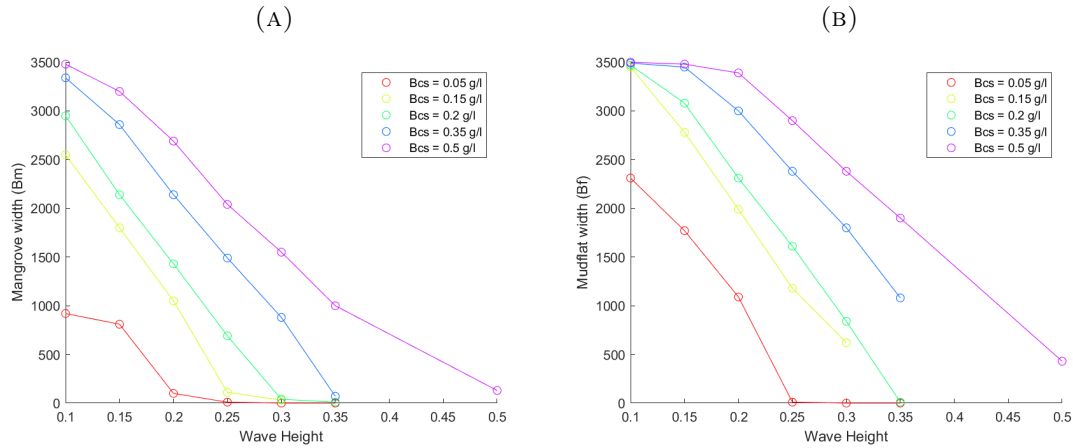
FIGURE 26: Width of mangroves and mudflat after 40 years of simulation in MFlat (A) Mangrove width (B_m) in meters at equilibrium after 40 years (B) Mudflat width (B_f) in meters at equilibrium after 40 years.

From these plots, it is shown that the mangrove- and mudflat width in MFlat decreases with a higher wave height, and that the mangrove- and mudflat width increases with a higher boundary condition of sediment. It also clearly shows the boundary of the model, as the mudflat width is restricted by the maximum width of the model, which is 3500 m.

Tidal prism

Besides the width of the mangrove/ mudflat areas, also the tidal prism is determined based on the equilibrium situation in MFlat. The relation between the wave height, the boundary sediment concentration and the tidal prism is presented in figure 27. For the computation of the tidal prism the same definition is used as in ShorelineM, i.e. the purple trapezium in figure 4, which determines how much water enters the areas above MSL. The tidal prism is calculated as the difference between MHW and the bed level at the mangrove area and is presented in figure 28.
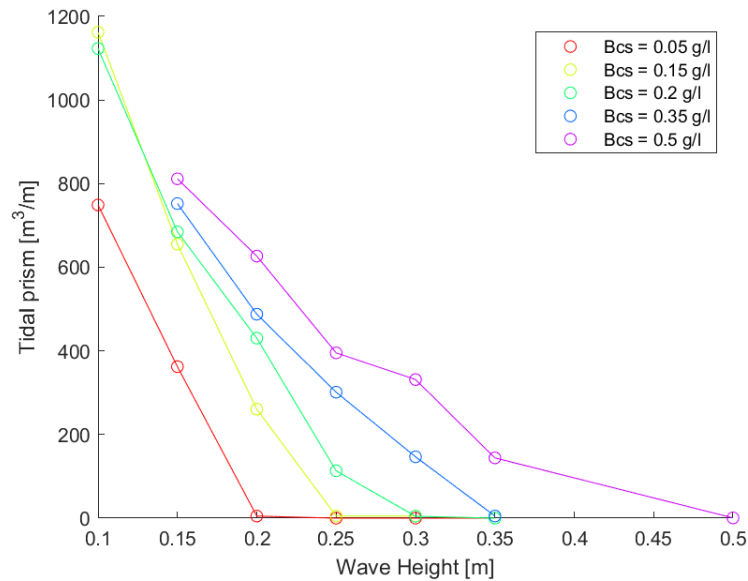
FIGURE 27: Tidal prism of the equilibrium situation after 40 years for different conditions.

45

The tidal prism increases for a higher boundary sediment concentration and decreases for a higher wave height. The tidal prism is also limited by the model domain and limited by the absence of SLR in the simulations. Towards the equilibrium situation, the volume of the tidal prism first increases and then decreases as bed levels are accreting towards MHW. This development of the tidal prism can be seen in the appendix in figure 55 for a wave height $H_{rms} = 0.50$ m and a boundary sediment concentration $c_{bcs} = 0.50$ g/l. As there is no SLR, the model is accreting towards MHW, which decreases the available volume for water in the mangrove area.

In the figure above, two conditions are missing (with a wave height $H_{rms} = 0.10$ m and a boundary sediment concentration $c_{bcs} = 0.35$ and 0.50 g/l). These two conditions did not result in a stable profile, as can be seen in the cross-shore profiles for a wave height $H_{rms} = 0.10$ m in Appendix A.3.2.

Cross-shore profile for a wave height of 0.20 m
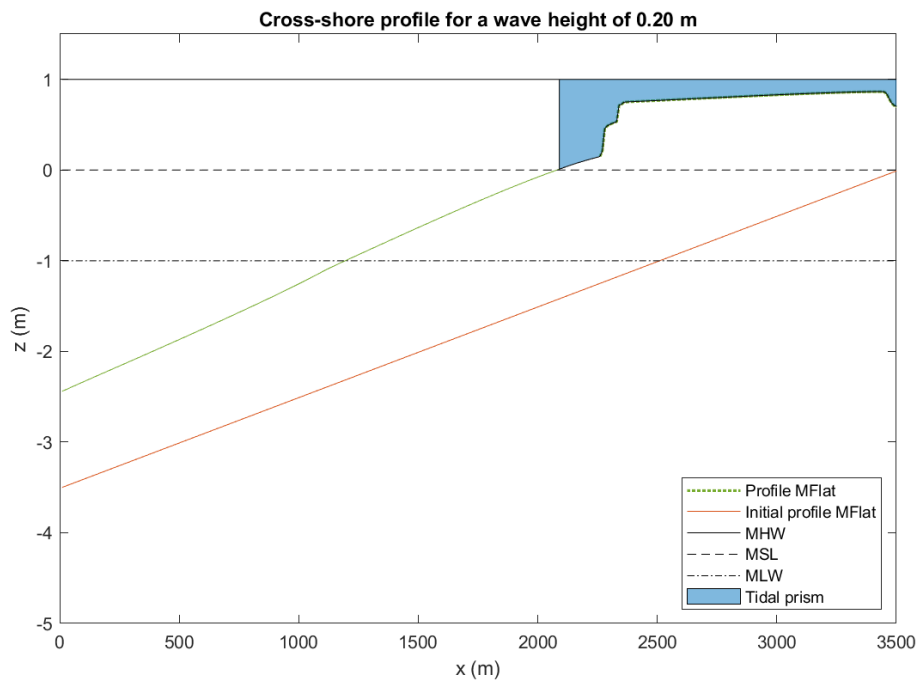
FIGURE 28: Definition of the area where the tidal prism is calculated, for the simulation with a wave height $H_{rms} = 0.20$ m and a boundary sediment concentration $c_{bcs} = 0.20$ g/l. The tidal prism is the volume of water that enters the mangrove area during one tide, and is calculated as the difference between MHW and the bed level at the mangrove area.

Sediment volume in mudflat/mangrove area

As the development of mangroves in ShorelineM is depending on volumes, also the volume of the mangrove- and mudflat area in MFlat is computed for the equilibrium situation, so it could be used in ShorelineM. The relation between the wave height, boundary sediment concentration and volume of mangrove area is presented in figure 29a, for the mudflat area it is presented in figure 29b. The volume of the mangrove area is defined as the area between the bed level and a 'reference line' which in this study is MLW. By using MLW, the volume of the mangrove area can be combined with the volume of the mudflat area, which reaches till MLW. The volume of the mangrove area is only calculated from the landward boundary till the lowest possible bed level before MSL, as can be seen in figure

30. The volume of the mudflat area is the sum of the volume of the mangrove area and the volume of the mudflat in front of the mangroves.
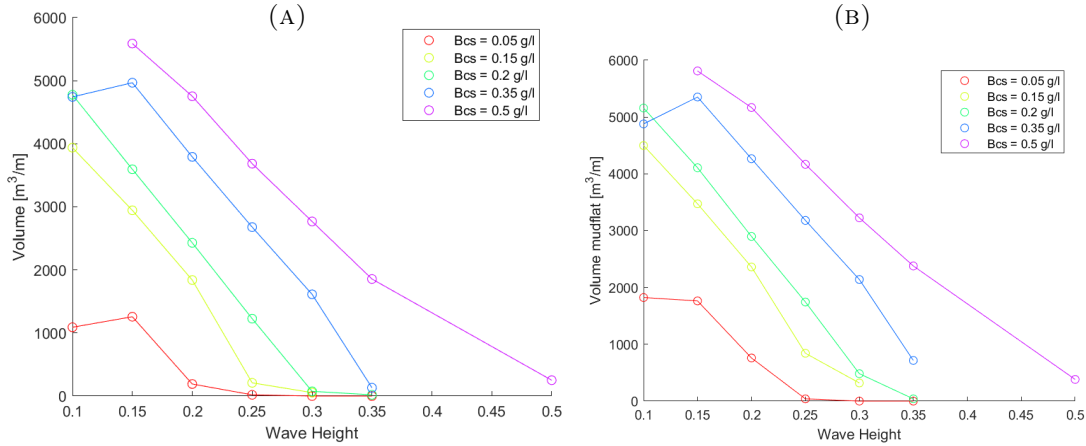
FIGURE 29: Volume of mangrove- and mudflat area after 40 years of simulation in MFlat for different conditions (A) Volume of mangrove area (B_m) at equilibrium after 40 years (B) Volume of mudflat area (B_f) at equilibrium after 40 years.

The volume of the mangrove area increases for a higher boundary sediment concentration and decreases for a higher wave height. The maximum volume that can be reached is 7000 m^3/m (maximum for a domain of 3500 m and MLW = -1.0 m due to the tidal amplitude of 1.0 m), which is not realistic and accurate as the entire model domain has accreted.
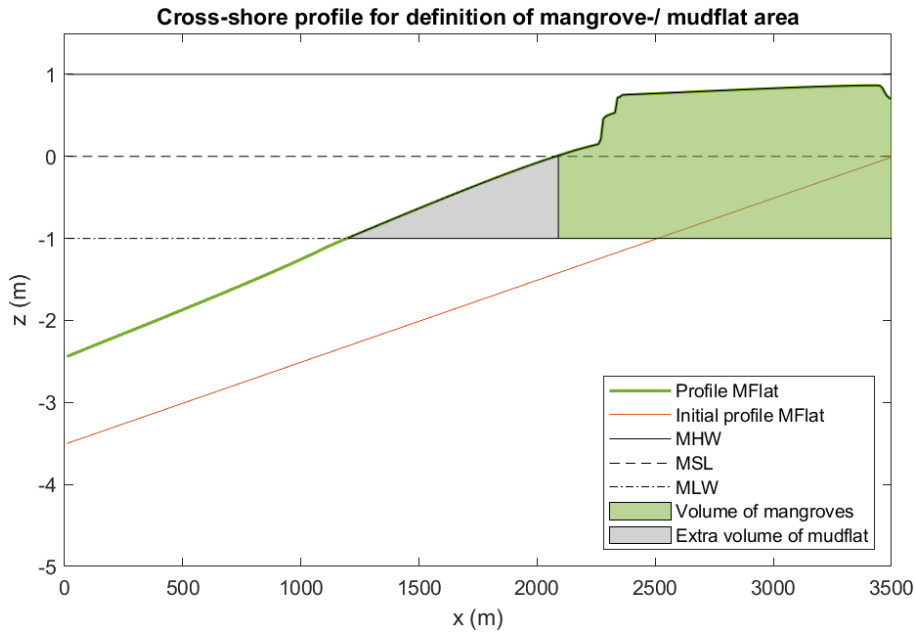
FIGURE 30: Definition of the area where the volume of the mangroves and mudflat is calculated. The mudflat area is the green area, whereas the mudflat area is the sum of the green and grey area.

4.2 Quantification of cross-shore fluxes

Along with analyzing the equilibrium situation at the end of the simulation, also information of the dynamic situation is used to determine cross-shore dynamics of mangroves. For this study, the characteristics that are determined are the cross-shore fluxes and the sediment trapping efficiency.

For analyzing this dynamic situation, 4 runs with a smaller time interval for saving the data were run. The 4 conditions below were simulated with a smaller time interval for saving, as these simulations resulted in a mangrove width of roughly 1500 m, which means that the mangroves were not influenced by the boundary of the model:

- $H_{rms} = 0.15$ m, $c_{bcs} = 0.05$ g/l
- $H_{rms} = 0.20$ m, $c_{bcs} = 0.20$ g/l
- $H_{rms} = 0.25$ m, $c_{bcs} = 0.35$ g/l
- $H_{rms} = 0.35$ m, $c_{bcs} = 0.50$ g/l.

4.2.1 Cross-shore fluxes

To define the cross-shore fluxes over the simulation period, the position where the flux is determined is changing over time. This happens as the lowest point of the mudflat/ mangrove is changing. In Matlab, this intersection of the bed level with MLW (B_f) and MSL (B_m) is computed per time interval for saving (dt = 10 minutes), which is then used in the computation of the cross-shore flux. The cross-shore fluxes are determined at two locations, and during two time periods, which results in four datasets for fluxes, see figure 31. The two locations are the transition from the foreshore area to the mudflat area B_f and the transition from the mudflat area to the mangrove area B_m. The two time periods are the ebb- and flood stages, defined by the water levels.
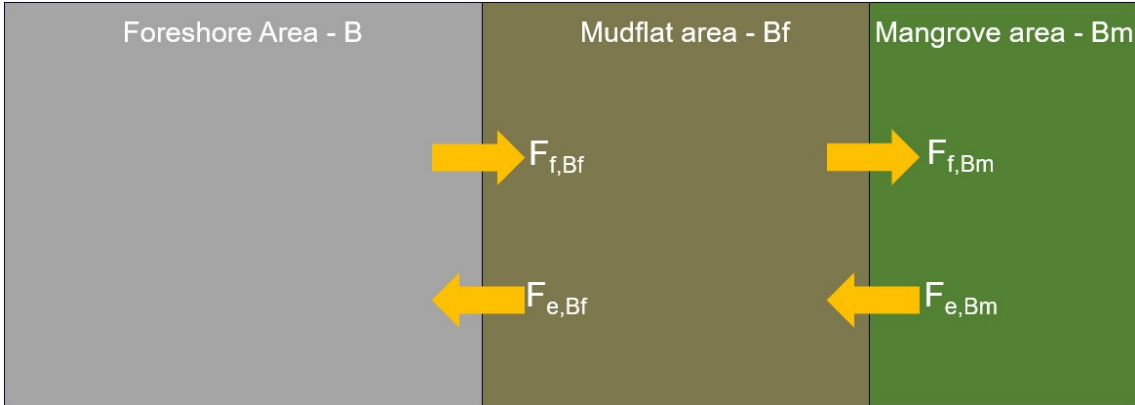
FIGURE 31: Schematization of the different fluxes used for determining the trapping efficiency. Where the fluxes during flood are defined by the subscript $_f$ and during ebb by the subscript $_e$.

At the locations mentioned above, the different fluxes are determined in MFlat. Figure 32 shows the fluxes during flood phase (when water levels increase from MLW to MHW) to the mudflat- and mangrove area. As with flood the water level is increasing, the fluxes are both positive and in landward direction. During the simulation, the width of the mudflat first increases, which increases the amount of sediment that passes the mudflat. When the mangrove area starts expanding, the mudflat area decreases in width, which also decreases

the flux towards the mudflat. The flux towards the mangroves starts when the mangrove area starts expanding. This flux is then quite stable over time.
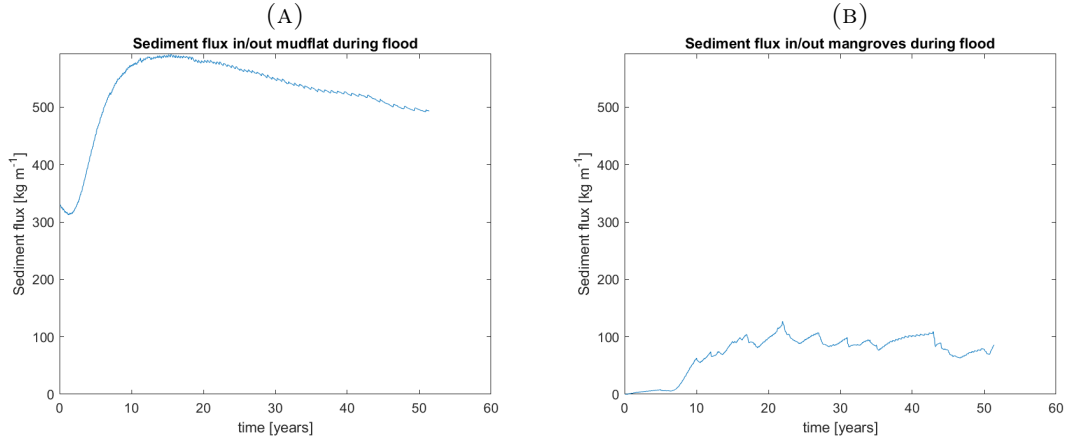
FIGURE 32: Sediment fluxes during flood phase at the moving position of the mudflat and the mangroves for a wave height $H_{rms} = 0.20$ m and a boundary sediment concentration $c_{bcs} = 0.20$ g/l. Positive fluxes are transported into the area. (A) Sediment flux passing the transition between foreshore- and mudflat area during flood phase. (B) Sediment flux passing the transition between mudflat- and mangrove area during flood phase.

For a wave height $H_{rms} = 0.20$ m and a boundary sediment concentration $c_{bcs} = 0.20$ g/l, figure 33 shows the fluxes during ebb phase (when water levels decrease from MHW to MLW) from the mudflat- and mangrove area. As with ebb the water level is decreasing, the fluxes are both negative and in seaward direction. Compared with the fluxes in the flood phase, the fluxes during ebb are smaller in an absolute sense. These fluxes are smaller, as sediment is deposited at the mudflat- and mangrove area, which is shown in figure 34.
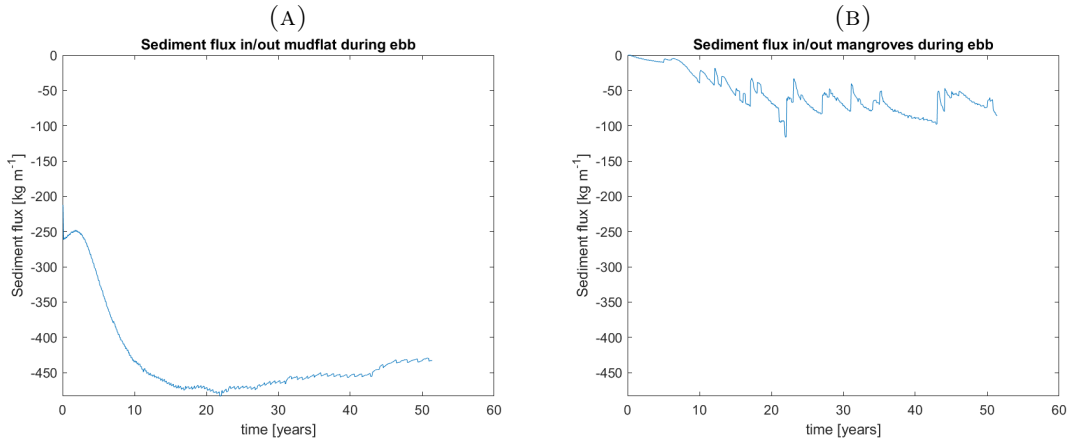
FIGURE 33: Sediment fluxes during ebb phase at the moving position of the mudflat and the mangroves for a wave height $H_{rms} = 0.20$ m and a boundary sediment concentration $c_{bcs} = 0.20$ g/l. Negative fluxes are transported out of the area. (A) Sediment flux passing the transition between mudflat- and foreshore area during ebb phase. (B) Sediment flux passing the transition between mangrove- and mudflat area during ebb phase.

The deposition that is plotted in the figures below is the difference between the fluxes in the flood phase and the ebb phase. On the transition from the foreshore area to the mudflat area, the deposition first increases rapidly, and increases slowly after roughly 10

years. In the mangrove area, the deposition increases after roughly 5 years, and decreases slowly after roughly 25 years.
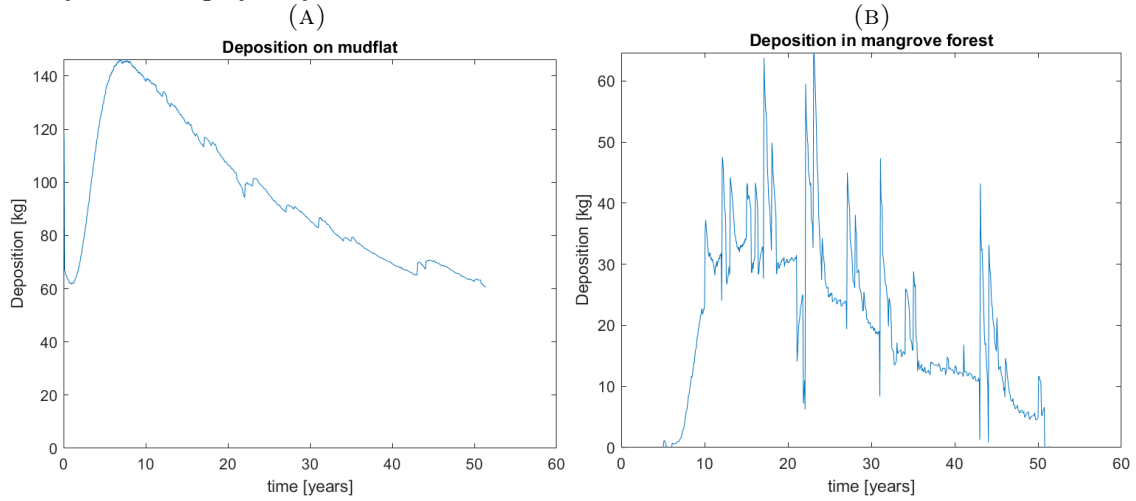
FIGURE 34: Sediment deposition in kilograms in the different areas (A) Sediment deposition in the mudflat area. (B) Sediment depostion in the mangrove area.

4.2.2 Sediment trapping efficiency

The next characteristic that is analyzed in MFlat is the sediment trapping efficiency. The trapping efficiency is determined by calculating the ratio of the sediment flux relative to the sediment deposition in the mangrove area, see Eq.(26). The deposition is the net difference between the sediment flux into the mangrove forest during flood and the sediment flux out of the mangrove forest during ebb. This is divided by the sediment flux into the mangrove forest.

$$STE = \frac{\text{Deposition mangrove forest}}{\text{Sediment flux into forest}} * 100\% \tag{26}$$

Where the deposition in the mangrove forest from figure 34b is used, and where the sediment flux into the mangrove forest from figure 32b.

For the four simulations that were executed with a smaller time interval, the sediment trapping efficiency is computed. The sediment trapping efficiency for the situation with a wave height $H_{rms} = 0.20$ m and a boundary sediment concentration $c_{bcs} = 0.20$ g/l is presented in figure 35, for the other situations the sediment trapping efficiency is presented in appendix A.3.3 .
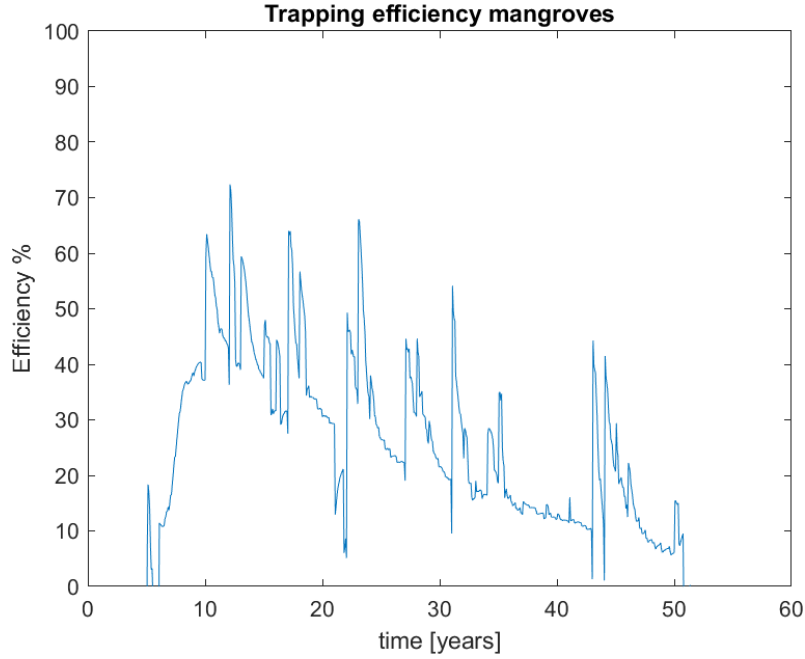
FIGURE 35: Sediment trapping efficiency over time for a wave height $H_{rms} = 0.20$ m and a boundary sediment concentration $c_{bcs} = 0.20$ g/l.

The sediment trapping efficiency for this situation increases after roughly 6 years towards 50% and decreases slowly (with some peaks in between) to an efficiency of roughly 10%. For the other situations the sediment trapping efficiency is presented in appendix A.3.3 with efficiencies of approximately 30%, 10% and -10%.

4.3 Answer to RQ2

MFlat successfully simulated the situation of mangroves after 40 years at the Guyana coast. Therefore the characteristics of mangrove forests (mudflat- and mangrove width) after 40 years of simulating could be used to implement cross-shore dynamics in ShorelineM. During the 40-year simulation, the cross-shore fluxes and sediment trapping efficiency are determined too (as it could be implemented in ShorelineM), showing significant variation and generally higher values than field data. However, as cross-shore fluxes were quite high and the sediment trapping efficiency ranged from roughly 50% to -10%, both were not taken into account for the coupling of ShorelineM and MFlat.

5   Implementing cross-shore dynamics in ShorelineM

As mentioned in the previous chapters, ShorelineM is lacking cross-shore sediment fluxes and trapping. The cross-shore model MFlat simulates these cross-shore dynamics and has shown that it reproduces reliable mangrove- mudflat profiles (Best et al., 2024). In this chapter, the cross-shore dynamics of MFlat are implemented in ShorelineM by using a library of simulation results with different conditions in MFlat. The cross-shore information that is used is the width of the mudflat- and mangrove areas and the formulation of the cross-shore profiles. First the set-up of the coupling is explained, this coupled model is then tested for the case study. The results of this coupled model for the case study are shown afterwards. Overall, this chapter aims to answer research question RQ3.

5.1   Cross-shore morphodynamics from MFlat

A look-up table was created containing cross-shore information for 31 conditions simulated in MFlat, see table 36. These simulations had a different wave height H_{rms} and a different boundary sediment concentration c_{bcs}, as presented in table 3. The look-up table contains information about the width of mudflat- and mangrove areas, the slope of these areas, the tidal prism and the shape of the cross-shore mudflat profile. The slope, tidal prism and shape of the profile are not used in this study, but can be used for future extensions of the model coupling (e.g. when a change of the profile shape is implemented). The shape of the mudflat profile gives extra information about the situation of the mudflat, i.e. if it is convex-up and more likely accreting or if it is concave-up and more likely eroding (Friedrichs, 2011). The shape of the mudflat is defined by dividing the slope of the mudflat halfway in two sections; if the slope of the landward side of the mudflat is more gentle than the seaward side, the profile is convex-up, if the slope of the seaward side of the mudflat is more gentle than the landward side, the profile is concave-up.

...	H_rms	c_bcs	B_f	B_m	SBf	SBm	P	shp
1	0.1000	0.0500	2310	920	7.3904e-04	2.8500e-04	749.0072	'Convex-up'
2	0.1000	0.1500	3450	2550	0.0013	2.1739e-04	1.1622e+03	'Convex-up'
3	0.1000	0.2000	3470	2950	0.0021	1.9509e-04	1.1232e+03	'Convex-up'
4	0.1000	0.3500	3490	3340	0.0074	-4.1092e-05	79.6898	'Convex-up'
5	0.1000	0.5000	3500	3480	0.0548	-2.1079e-04	6.3108	'Concave-up'
6	0.1500	0.0500	1770	810	0.0010	8.5601e-04	362.3449	'Concave-up'
7	0.1500	0.1500	2780	1800	0.0011	3.2837e-04	655.4138	'Convex-up'
8	0.1500	0.2000	3080	2140	0.0012	2.7606e-04	684.8414	'Convex-up'
9	0.1500	0.3500	3450	2860	0.0021	2.0285e-04	752.3519	'Convex-up'
10	0.1500	0.5000	3480	3200	0.0040	1.7421e-04	811.5428	'Convex-up'
11	0.2000	0.0500	1090	100	0.0011	0.0081	4.9525	'Concave-up'
12	0.2000	0.1500	1990	1050	0.0011	7.0189e-04	260.5946	'Concave-up'
13	0.2000	0.2000	2310	1430	0.0012	4.8563e-04	430.4631	'Convex-up'
14	0.2000	0.3500	3000	2140	0.0014	2.7695e-04	487.7030	'Convex-up'
15	0.2000	0.5000	3390	2690	0.0019	2.0987e-04	626.7075	'Convex-up'
16	0.2500	0.0500	10	10	0.0013	-2.0722e-06	1.0361e-04	'Concave-up'
17	0.2500	0.1500	1180	110	0.0010	0.0089	5.0500	'Concave-up'

FIGURE 36: Look-up table in ShorelineM, with data of the cross-shore morphodynamics in MFlat.

The table is used to determine the four conditions that are closest to the simulated conditions (H_s and $\bar{c}$) in the ShorelineM simulation and to find corresponding values for the width of the mudflats (B_f) and mangroves (B_m). So, for example with a wave height

$H_s = 0.17$ m, and a sediment concentration $\bar{c} = 0.25$ g/l in ShorelineM, the values of B_f & B_m of rows 8, 9, 13 & 14 are used. With linear interpolation, the corresponding value is determined and this value is divided by the number of simulation years (40 years) to determine the change of mangrove and mudflat width ($\frac{dB_m}{dt}$ & $\frac{dB_f}{dt}$). If the exact wave height or sediment supply is simulated in ShorelineM, the exact value from the table is used (which then uses only two rows from the table).

5.2 Results from idealized testcase for a schematized mudflat inspired by Guyana conditions

5.2.1 Results for constant conditions

As mentioned before, the option that is researched during this study, is the option with the updated development of the width from MFlat (with Eq.(22)). Simulating this over a period of 40 years, results in an increase of the shoreline width of roughly 2.5 kilometers at the location of the river input, as visible in figure 37. As the wind and waves are coming from the southeast, the sediment is distributed along the coast in northern direction. The development over time for this situation at the location of the river input is visible in figure 38.
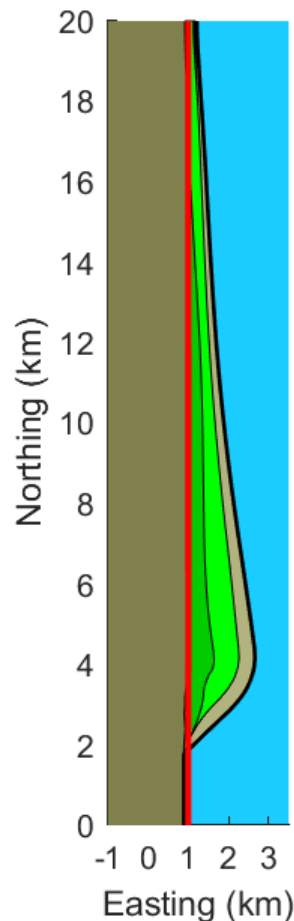
FIGURE 37: Predicted shoreline development after 40 years of simulation with Eq.(22) and the updated mangrove width from MFlat in ShorelineM with constant sediment input at one location (N = 4km).
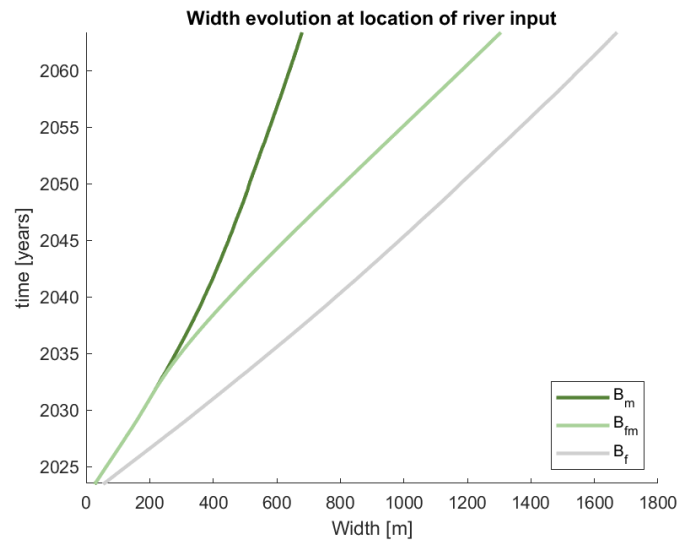
FIGURE 38: Evolution of width of the different areas at the location of the river input at N = 4 km.

5.2.2 Results for cyclic conditions

In the situation with cyclic sediment conditions, the shoreline width increases mostly at the northern part of the model domain, which can be seen in figure 39. The maximum increase of the shoreline width is roughly 1.0 km. The evolution of the three different zones is shown in figure 40. The width of the mangrove forest increases towards 400 m, whereas the mudflat width increases towards 1000 m. After 10 years, the mangrove width is roughly 200 m. This corresponds with the situation at the Guyana coast, where the forest fringe has developed ranging from 120 to 400 m after 10 years (Best et al., 2022a).
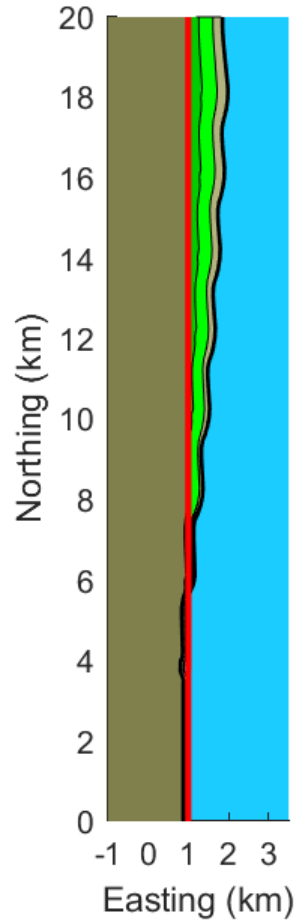
FIGURE 39: Overview of the development after 40 years of simulation with cyclic conditions.
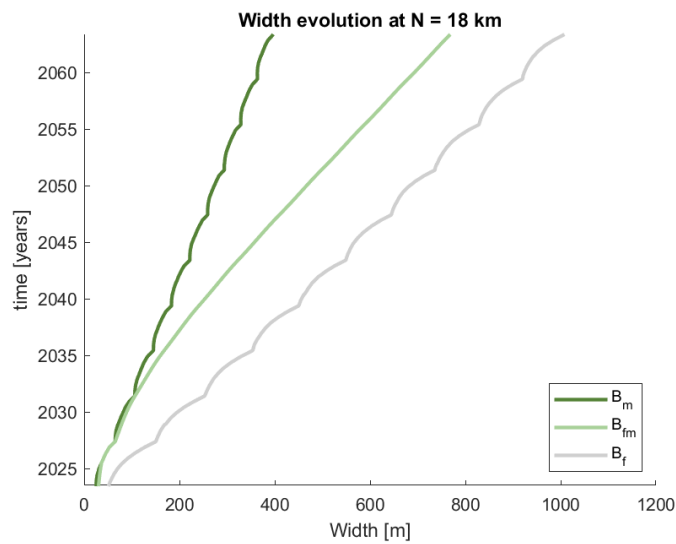
FIGURE 40: Evolution of width of the different areas at the location at N = 18 km for cyclic sediment conditions.

5.2.3 Comparison testcases

To show the differences between the two testcases, the development of the width at the two locations from figure 38 and 40 are shown in figure 41.

Compared with the situation at the coast of Guyana, the cyclic conditions better represent the shape of coastline, as shown in figure 13. At the coast of Guyana, the mangrove belt has a width varying from 100 to 400 meter after 10 years (Best et al., 2022a). At the location at N = 18 km, the results show a mangrove width of roughly 200 m after 10 years. The shape of the coastline also corresponds with the situation at Guyana, as the highest increase of the shoreline width occurs at the Northern part of the model/ domain. The conditions with steady sediment input at one location resulted in a situation with a huge increase of the shoreline width at that location, whereas this shoreline width decreases towards the North. Also the width at the location of the river input is much higher than the width at the Guyana coast. Therefore, the situation with constant sediment input is not used, as it does not represent the situation at the coast of Guyana.
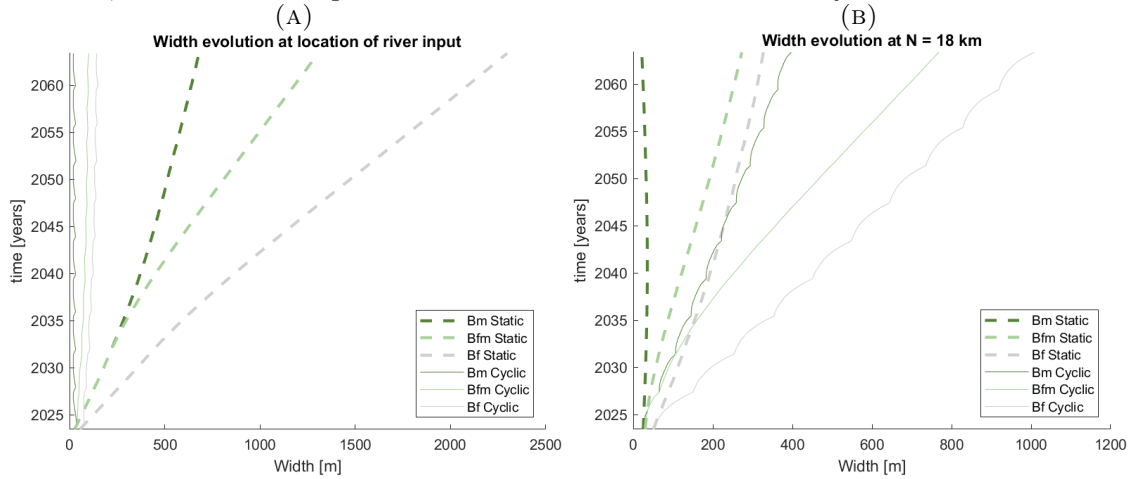
FIGURE 41: Comparison of width evolution of both cases (A) Width evolution at the location of sediment input for the constant river discharge at N = 4 km (B) Width evolution at N = 18 km, close to the model boundary.

5.3 Answer to RQ3

In the two cases that were studied, with a constant sediment input and cyclic sediment input, the model shows accurate results without model instabilities. By including cyclicity in the sediment input, the shape of the mangrove area and coastline corresponds with the situation at the coast of Guyana. For a constant sediment input, the shape of the coastline and the mangrove area does not represent the situation at the coast of Guyana.

6 Discussion

In this study the goal was to improve the model capability of ShorelineM to predict the long-term development of mangrove-mud coastlines by coupling it to the cross-shore model MFlat. From MFlat, information about the width of the mangrove-/ mudflat area for different conditions is implemented in ShorelineM. The coupled model shows dynamics that represent the situation at the coast of Guyana. However, there is still a number of issues to be addressed before the model can be used to determine the long-term development of mangrove forests for 50 to 100 years.

6.1 Comparison of original model and case study

The scenarios that are run in section 5.2 result in simulations with a maximum increase of the shoreline width of roughly 1600 meters for constant sediment input and a maximum increase of roughly 1000 meters for cyclic sediment input over a period of 40 years. The mangrove forest area for the constant sediment input maximally expands around 600 m after 40 years, whereas for the cyclic sediment input the mangrove forest area maximally expands to around 400 m. Over a time period of 10 years (2011-2021), the forest fringe at the Guyana coast has developed a width ranging from 120 to 400 meter (Best et al., 2022a). The situation with cyclic conditions (see figure 40) corresponds with the situation at the Guyana coast, as the forest fringe in this situation has a width of roughly 200 meter at N = 20 km after 10 years.

In figure 42 the result of the original model for the cyclic conditions are visible, as these results from the updated model represented the situation at Guyana the best. With these conditions, the increase of the shoreline width is bigger than in the new model and model instabilities occur at the boundary of the model (at N = 21 km). The difference between the development of the width for the updated model and the original model are visible in figure 43 at the location at N = 18 km. In the original model, this results in a linear development over time. However, in this situation model instabilities occur at the Northern part of the model, which is visible in the overview of figure 42.

The biggest difference between the original model and the updated model is the longshore- and cross-shore distribution of sediment. Within the original model all the sediment input resulted in an increase of the shoreline or is transported out of the domain, whereas in the new set-up the sediment concentration determines the change of width of the areas based on MFlat and sediment can be transported along the coast. The width is then based on the cross-shore profile from MFlat, where sediment is accreting the profile. The cross-shore distribution of sediment is therefore different in the updated model, which slows down the development of the mangroves and mudflats. The sediment input by the river in ShorelineM then only increases the suspended sediment concentration in front of the coast, which determines the change of width of mangroves and mudflats over time based on the MFlat simulations.
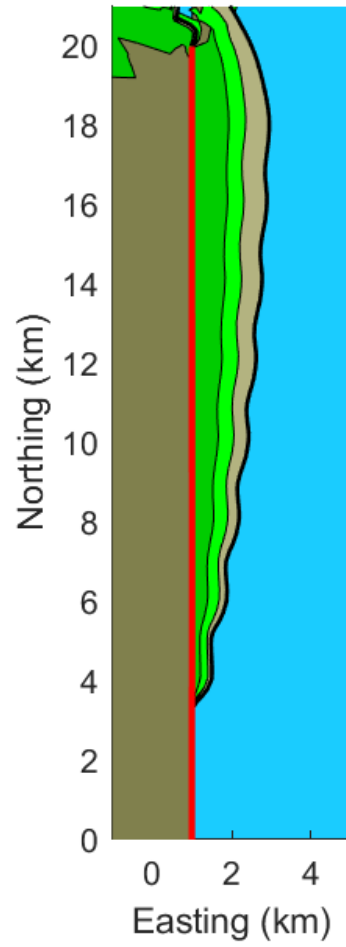
FIGURE 42: Shoreline prediction in original ShorelineM model after 40 years of simulation with cyclic conditions.

Width evolution at N = 18 km
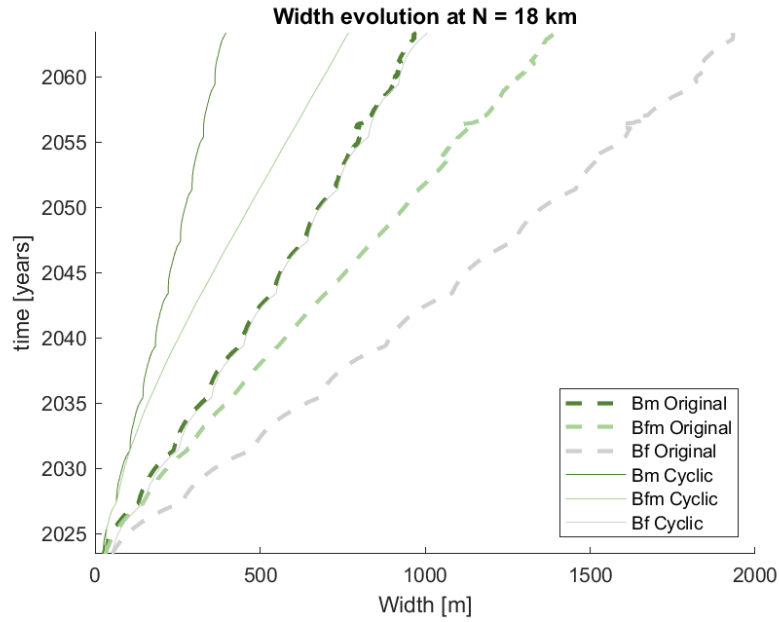
FIGURE 43: Comparison of width evolution of original and updated model with cyclic conditions at N = 18 km, close to the model boundary

In reality, the observed sediment concentrations at the Guyana coast (40-60 g/l) are higher than the modeled sediment concentrations in MFlat (with a maximum of 4 g/l) (Best et al., 2024) and in ShorelineM (with a maximum around 1 g/l. With higher concentrations in MFlat, the domain filled up too fast, which resulted in unstable simulations and is caused by the absence of fluid mud in MFlat. This is the same in the updated ShorelineM model, as the entrainment of sediment is only caused by currents, which causes lower sediment concentrations based on the actual conditions. The actually observed sediment concentrations at the Guyana coast may be the result of fluid mud, which can dissipate wave energy and increases the accretion of the profile (Best et al., 2024). However, this process is not included in both models and therefore simulated concentrations are lower.

6.2 Relevance of the coupled model for long-term development

The coupling of both models provides more information of how the sediment is distributed in cross-shore direction and how this develops the width of the mangrove area over time. As this development is based on the simulations in MFlat, the vegetation dynamics (establishment, growth and death of vegetation) is included in the model. Another advantage of the coupled model is that the computational time is quite small (1-10 minutes). Therefore it is easy to run multiple different scenarios with changes in hydrodynamics and sediment dynamics. If the model is calibrated (by using the hydrodynamic and sediment data and mangrove characteristics collected at the Guyana coast during multiple weeks (Best et al., 2022a)) for bed levels and the vegetation height and density and validated (by using hydrodynamic and sediment data from another location for a similar period of multiple weeks, e.g. Ca Mau or Firth of Thames) the model can also be used for other locations. After further improvements of the model (change of profile shape, including fluxes from MFlat), the model could be helpful for organizations or governments to simulate multiple scenarios for the long-term development of mangrove-mud coastlines, which can be used for the coastal zone management.

The simulations with the model were run with a maximum of 40 years, as within this time period MFlat produces an equilibrium profile. In cases with a high boundary sediment concentration ($c_{bcs} = 0.35$ g/l & 0.50 g/l) the equilibrium forms after roughly 30 years, whereas for cases with a lower sediment concentration the model is growing towards an equilibrium with some small changes after 40 years. The testing in ShorelineM was limited to 40 years, so that the same time period of the MFlat simulations was used.

However, to determine trends in the long-term development of mangrove forests based on changes in sediment supply or water level, this period is probably too short and should be increased to 60 to 100 years for defining an equilibrium situation based on new conditions (e.g. faster wind velocities). The simulated periods in ShorelineM needs to be extended then, where still the results of the situation after 40 years from MFlat can be used.

6.3 Temporal variability of boundary conditions

6.3.1 Cyclicity in sediment input

In the MFlat results used for this study, no temporal variability is included and only a constant value for the wave height and sediment boundary condition is taken into account. By this manner, MFlat simulations converge to an equilibrium situation, which is formed after approximately 40 years. However, along the coast of Guyana, the sediment input differs over years, depending on the sediment fluxes from the Amazon (Best et al., 2022b). This cyclicity in sediment input makes the equilibrium a dynamic equilibrium.

6.3.2 Wave height

Also, a single value of the peak wave period is used, whereas in reality there is not really one peak value. This wave condition should represent the wave spectrum and energy of the waves (Ntriankos, 2021). Normally, the full wave spectrum should be used, which influences the development of the mangrove forests (e.g. transport more sediment into the mangroves or damage the mangrove trees). However, this is not possible in MFlat (Ntriankos, 2021).

6.3.3 Storms

Tropical storms and hurricanes are not taken into account in this study. This was taken into account in the report of Ntriankos (Ntriankos, 2021), yet only for a short period of time (e.g. one or multiple days). As in that study storm events were included in the simulations, the wave heights and periods were increased towards 1.0 meter and 6-8 seconds for a short period of time (e.g. one to two days). This increased the sediment input in the mangrove area, but also damaged some of the mangrove trees. When including storms in the coupled model, it may cause instabilities in the model, as the original ShorelineM-model faces problems with wave heights higher than 0.75 meter.

6.4 Sea Level Rise

In the current version of ShorelineM, sea level rise could not be implemented accurately and is therefore not taken into account in the simulations. To couple both models, the conditions should be set up the same way and SLR should be implemented in both models or not. Therefore, SLR was switched off in MFlat. For the long term mangrove development (50 to 100 years), it is however important to take SLR into account, as according to the

RCP8.5 scenario of the IPCC the expected SLR in 2100 is between 61 and 110 centimeters (Intergovernmental Panel on Climate Change, 2022).

Implementing SLR in the simulations will change the results of both models, depending on the chosen scenario. In situations without SLR, the tidal prism decreases over time as less space is available trough accumulation in the forest. In simulations with SLR, the tidal prism increases again, as with an increasing water level more water could enter the forests (Xie et al., 2022). This increasing tidal prism can change the results positively and negatively, as in one way more sediment can enter the forest, which increases the bed levels and compensates SLR. However, in the other way the inundation period increases, which increases the possibility of the death of mangrove trees (van Maanen et al., 2015) and the increasing tidal prism can cause erosion due to increased flow velocities.

6.5 Sediment trapping efficiency

Determining the sediment trapping efficiency with MFlat had some difficulties, which in some way also occurs when determining it in the field (where other difficulties are faced due to turbulence of water over the sediment traps). In the field, the amount of sediment that is captured during one tidal cycle is measured with sediment traps (Horstman et al., 2015; Chen et al., 2018). The flux into the mangrove area can be calculated from the concentration, water depth and flow velocity, for which the sediment concentration can be measured at different water depths (Chen et al., 2018; Best et al., 2022a). In MFlat, the trapped sediment is determined based on the difference between in- and outflow of sediment, which is determined based on the water depth, flow velocity and sediment concentration. In MFlat, the simulated concentration is a depth averaged sediment concentration. MFlat also uses a depth-averaged velocity, which affects the shear stresses and erosion and underestimates the actual suspended sediment concentration (Baird, 1999). Because of the definition of trapped sediment and the depth averaged velocity, the sediment trapping efficiency for a wave height $H_{rms} = 0.35$ meter and a boundary sediment concentration $c_{bcs} = 0.50$ g/l (appendix A.3.3) shows negative values only, which does not represent the accreting coastline in that situation. For the definition of the trapped sediment, the settling and resuspension of sediment is not taken into account, which could cause the negative values for the sediment trapping efficiency.

Also the tidal symmetry in MFlat makes the computation of the sediment trapping efficiency incorrect. The cross-shore velocities in MFlat are symmetrical by assumptions in the model (see figure 11a), whereas tidal asymmetry would be expected as in reality. This affects the amount of sediment that is transported into the mangrove forests during flood phase and the amount of sediment that is deposited after a tidal cycle. As the velocities during ebb phase are of the same order as during flood phase, more sediment is resuspended and can be transported out of the mangrove area (Chernetsky et al., 2010), whereas normally ebb currents are weaker than flood currents.

The above mentioned factors also result in differences in the cross-shore fluxes determined in MFlat compared to the cross-shore fluxes determined by the field observations by Chen et al. (2018) in the Yunxiao National Mangrove Reserve, located at the Zhangjiang Estuary. With a suspended sediment concentration $c = 0.05$ g/l and a maximum cross-shore velocity $u = 0.10$ m/s at the mangrove edge, the net cross-shore flux measured by Chen et al. (2018) is 3.2 kg/m per tidal cycle. For a similar situation in MFlat, with a boundary sediment concentration $c_{bcs} = 0.05$ g/l and a wave height $H_{rms} = 0.15$ m, the cross-shore fluxes during one tidal cycle are a factor 10 larger, as is visible in figure 44 . In this situation, the maximum cross-shore velocity $u = 0.4$ m/s, what may cause the difference in sediment flux. For the other simulated situations with higher sediment

concentrations, the sediment flux in MFlat is even higher, see figure 32b.
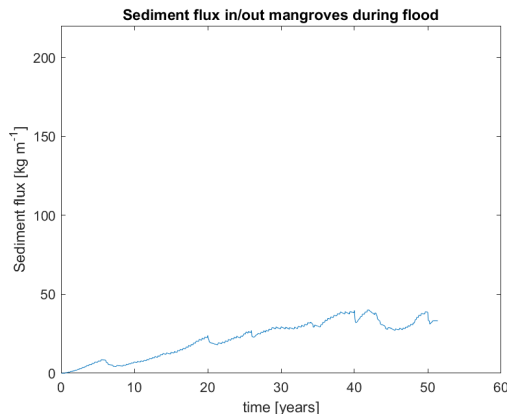
FIGURE 44: Sediment flux into mangrove forest during flood phase for a wave height H_{rms} of 0.15 m and a boundary sediment concentration c_{bcs} of 0.05 g/l.

6.6 Initial profile width in MFlat

As the results of the updated model are only focused on one location, the results can vary a lot on other locations. The Guyana coast is characterized by mudflats with a width of several kilometers (Best et al., 2022b). These mudflats originate from the mudbanks that move along the coasts of South America and which are driven by suspended sediment from the Amazon river. Through these mudbanks, the intertidal area in front of Guyana can be characterized by its mild slope (1/1500 or 0.00066 m/m) which is quite mild compared to other intertidal areas with slopes of roughly 1/200 to 1/1000 or 0.006 to 0.001 m/m (Xie et al., 2022). In MFlat, the width of the model was limited to 3500 meter in the simulations, as this corresponds the width of the mudflats at the Guyana coast, with an initial slope of 1/1000. In some cases (e.g. a boundary sediment concentration $c_{bcs} = 0.50$ g/l and wave height $H_{rms} = 0.15$ m) this resulted in a situation where most of the model was mangrove area, with just a small mudflat in front, therefore this situation is not accurate as it is limited by the boundary and could not develop further.

Apart from the mild slope, the results of the MFlat simulations also show different cross-shore profiles of the mangrove forests (see figure 24) than cross-shore profiles of forests that are measured at different locations around the world and which were visualized by Bryan et al. (2017) and Xie et al. (2022). In the results of MFlat, the cross-shore profiles of mangrove forests are quite smooth (with typical slopes of 1/1200 to 1/1500) and the forest fringe is fronted by a cliff that separates the mangroves with the mudflats, whereas slopes in field observations vary from 1/200 to 1/1000. The results also show that mangroves tend to grow towards mean sea level. However, in measurements at other locations (Xie et al., 2022), the mangroves can even grow below mean sea level or only at higher elevations.

In the simulations, only one initial profile with a slope of 3.5/3500 is studied. It is also possible to do simulations with multiple slopes to see how the mangroves react in different regimes (Xie et al., 2022).

6.7 Alternative methods to extend the capability of ShorelineM

Instead of using the information of the mangrove width from MFlat, it is also possible to use other sources of information to incorporate cross-shore dynamics into ShorelineM.

These sources cover other processes (e.g. the actual vegetation dynamics), that result in other outcomes, that may be more accurate and useful.

6.7.1 Machine learning

A possibility to implement the full cross-shore dynamics of MFlat (or an other model/ field data) into ShorelineM, is by incorporating machine learning. A method of machine learning is a neural network, where results are used to train a network to retrieve a certain relation. When the network is trained and tested, this network can for example be used to determine the relation between the hydrodynamic and sediment conditions with the development of the mangrove forests. The output of MFlat (multiple simulations) and the used parameters will be used to train and test the model. The output that should be used is the development of the width, volume and slope of the areas, the tidal prism and the vegetation properties (i.e. height, diameter, biomass). By testing and training the model, it should reproduce the same bed levels based on the given conditions (time series of hydrodynamic and sediment conditions).

6.7.2 Real-time coupling of models

Another possibility that could be used, is a real-time coupling of a cross-shore model (e.g. MFlat) with the longshore model ShorelineM, which will then be a Quasi-2D model. With this kind of coupling, the cross-shore dynamics and distribution of sediment from MFlat can be implemented into ShorelineM, which gives dynamic information and therefore updates both models. ShorelineM can then inform MFlat about the longshore distribution and availability of sediment. Disadvantages of such a coupling are the increase in computational time and the differences in processes (e.g. the inclusion of a MorFac and differences in volumes). An example of such a coupling is the LX-shore model, which focuses on sandy coasts only (Robinet et al., 2020).

7 Conclusions and Recommendations

The research was conducted based on the research questions mentioned in chapter 1. Below, the answer to the questions are presented:

7.1 Limitations ShorelineM

RQ1: How are current model assumptions in ShorelineM limiting the cross-shore development?

Simulations in ShorelineM show the potential of the model for determining long-term longshore development of mangrove-mud coastlines. However, it needs further improvements to achieve results that are more realistic. Model improvements in ShorelineM should be made in the conservation of the cross-shore profile, entrainment of sediment, the representation of the area of the cross-shore profile that faces inundation and the cross-shore sediment fluxes.

The cross-shore profile that is used in ShorelineM causes that all the sediment input results in an increase of the width of the mangrove-/ mudflat area. However, in real life this sediment can also change the cross-shore profile of the coastline so that it results in a convex-up or a concave-up profile. To achieve this, the cross-shore profile should be parameterized with a flexible bed level along the profile. This is not implemented in the model, but could be an useful improvement. By doing this the bed level of the mangrove- and mudflat area can be changed on multiple locations in cross-shore direction (instead of one uniform slope along the area), which makes it possible to form more realistic cross-shore profiles (i.e. convex-up and concave-up). If bed level changes are implemented in ShorelineM, it changes the cross-shore distribution of sediment and may slow down the expansion of the shoreline.

7.2 Dynamics and system dynamics MFlat

RQ2: How do the cross-shore profiles of mangrove forests develop on the long-term (up to 40 years) in the mangrove model MFlat for an idealized testcase in Guyana?

The cross-shore dynamics (i.e. cross-shore fluxes and profile changes) in ShorelineM are improved by implementing the cross-shore mangrove growth model MFlat. This model has already demonstrated realistic simulations of cross-shore dynamics along the Guyana coast (Best et al., 2024). In the MFlat model, the cross-shore profiles of mangroves forests are growing towards an equilibrium after roughly 40 years of simulating (depending on the initial situation and with absence of longshore dynamics). For different wave heights (H_{rms} = 0.10 - 0.50 m) and a different boundary condition of sediment at the seaward boundary of the model (c_{bcs} = 0.05 - 0.50 g/l), this results in different cross-shore profiles with different characteristics. Conditions with a low wave height and a high sediment concentration, result in a large width of the mangrove area, whereas conditions with a high wave height and low sediment concentration result in a small width or the absence of a mangrove area.

Besides this equilibrium situation, also the dynamic situation during the 40 years of simulation is used to determine the cross-shore fluxes towards the mangrove area and the sediment trapping efficiency in the mangrove area. The cross-shore fluxes are determined based on the cross-shore velocity, the water depth and the suspended sediment concentration. These computed cross-shore fluxes vary from 30 to 90 kg per meter width per tidal

cycle, which is a factor 10 larger than fluxes from field data. The cross-shore dynamics are also used to compute the sediment trapping efficiency in mangrove areas. This efficiency is computed based on the simulated sediment flux into and out of the mangrove forest and the deposition in the forest. For four accreting coastline situations ($H_{rms} = 0.15, 0.20, 0.25$ & 0.35 m and respectively $c_{bcs} = 0.05, 0.20, 0.35$ & 0.50 g/l), the efficiency ranged from roughly 50% to roughly - 10%. In accreting situations, it is expected that the sediment trapping is positive, as more sediment accretes than it is transported out of the area. However, in the last situation, the average sediment trapping efficiency is negative, and is therefore not used for the implementation in ShorelineM as probably settling and resuspension of sediment is lacking in the calculation.

7.3 Applicability to an idealized testcase

RQ3: To what extent improves coupling cross-shore dynamics from MFlat the longshore model ShorelineM for an idealized testcase in Guyana?

The information of the mudflat- and mangrove width from the simulations of MFlat are used to inform ShorelineM about the development of both areas based on the sediment concentration and wave height. The development of the MFlat simulations are stored in a look-up table, which is used in ShorelineM.

The mangrove- and mudflat width is divided by the simulation time of the MFlat simulations (i.e. 40 years), to get the change of width over time, which results in linear development.

For this implementation, a scenario with cyclic sediment input along the coast was studied. In this scenario, the model produces results that correspond the situation at the Guyana coast, with a mangrove width of roughly 200 meter in the Northern part of the model domain after 10 years, which corresponds with the mangrove width at the Guyana coast (Best et al., 2022b).

The integration of MFlat's cross-shore dynamics into ShorelineM is applied to a schematized mudflat inspired by conditions in Guyana. For a simulation with a simple schematization of the location, the results look promising and do not show model instabilities. However, as indicated in chapter 2.3.2, the mudflats in this test case are schematized and not representative of a specific moment in time due to the variability in mud fluxes, sediment input, and hydrodynamics at this location in Guyana.

7.4 Extension of the model / future research

To further improve the model capacity for predicting long-term development of mangrove-mud coastlines, the model has to be extended. This should be done by parametrization of the bed-levels of the cross-shore profile, coupling of the tidal prism and profile shape from MFlat to ShorelineM and implementing a non-linear relationship from the cross-shore dynamics of MFlat. Also other scenario's (with a different slope and a time variations of the wave height) from MFlat should be included, which extends the number of simulations. These simulations can be combined with possibilities for machine learning, so that the generated code from machine learning predicts the development of mangrove forests based on MFlat.

Also, the ShorelineM model should be calibrated on the bed levels and vegetation height and density by using the data collected by Best et al. (2022a) and validated by using data of another location (e.g. Ca Mau peninsula). After further improvements of the model (change of profile shape and including fluxes from MFlat) the calibrated- and validated

model may reproduce coastlines that correspond to the collected data. Then the model can be used by organizations and governments for coastal planning.

The ShorelineM-model was now only tested for a case with a simple geometry. The updated model should also be tested for different other cases, like situations where mangroves grow in a bay (e.g. Firth of Thames), or on a peninsula (e.g. Ca Mau). At these locations the coastline includes curvature, which is a challenge to get the model functioning accurate at locations where there is a bend in the coastline.

References

Aluri, J. S. R. (2013). Reproductive ecology of mangrove flora: Conservation and management. *Transylvanian Review of Systematical and Ecological Research*, 15:133–184.

Augustinus, P. (1978). The changing shoreline of suriname. *Natuurwetenschappelijke studiekring voor Suriname en de Nederlandse Antillen.*

Baird, W. (1999). Sediment trap assessment on sheboygan river and harbor. *USACE.*

Best, U. S. N., Legay, A., Reyns, J., and van der Wegen, M. (2024). Guyana mangrove-mudflat dynamics: Are coastlines formed by migrating mudbanks more resilient to sea level rise? Submitted for publication to Frontiers at 2024.

Best, U. S. N., van der Wegen, M., Dijkstra, J., Reyns, J., van Prooijen, B., and Roelvink, D. (2022a). Overview of datasets on advancing resilience measures for vegetated coastlines (arm4veg), guyana.

Best, U. S. N., van der Wegen, M., Dijkstra, J., Reyns, J., van Prooijen, B. C., and Roelvink, D. (2022b). Wave attenuation potential, sediment properties and mangrove growth dynamics data over guyana's intertidal mudflats: assessing the potential of mangrove restoration works. *Earth System Science Data*, 14(5):2445–2462.

Bryan, K. R., Nardin, W., Mullarney, J. C., and Fagherazzi, S. (2017). The role of cross-shore tidal dynamics in controlling intertidal sediment exchange in mangroves in cù lao dung, vietnam. *Continental Shelf Research*, 147:128–143. Sediment- and hydro-dynamics of the Mekong Delta: from tidal river to continental shelf.

Bunting, P., Rosenqvist, A., Hilarides, L., Lucas, R. M., Thomas, N., Tadono, T., Worthington, T. A., Spalding, M., Murray, N. J., and Rebelo, L.-M. (2022). Global mangrove extent change 1996–2020: Global mangrove watch version 3.0. *Remote Sensing*, 14(15).

Chan, S. C. Y., Swearer, S. E., and Morris, R. L. (2024). Mangrove cover and extent of protection influence lateral erosion control at hybrid mangrove living shorelines. *Estuaries and Coasts*, 47:1517–1530.

Chen, Y., Li, Y., Thompson, C., Wang, X., Cai, T., and Chang, Y. (2018). Differential sediment trapping abilities of mangrove and saltmarsh vegetation in a subtropical estuary. *Geomorphology*, 318:270–282.

Chernetsky, A. S., Schuttelaars, H. M., and Talke, S. A. (2010). The effect of tidal asymmetry and temporal settling lag on sediment trapping in tidal estuaries. *Ocean Dynamics.*

Friedrichs, C. (2011). Tidal flat morphodynamics: A synthesis. *Treatise on Estuarine and Coastal Science*, 3:137–170.

Fromard, F., Puig, H., Mougin, E., Marty, G., Betoulle, J.-L., and Cadamuro, L. (1998). Structure, above-ground biomass and dynamics of mangrove ecosystems: New data from french guiana. *Oecologia*, 115:39–53.

Gijsman, R., Horstman, E. M., van der Wal, D., Friess, D. A., Swales, A., and Wijnberg, K. M. (2021). Nature-based engineering: A review on reducing coastal flood risk with mangroves. *Frontiers in Marine Science*, 8.

Global Mangrove Alliance (2022). The state of the world's mangroves.

Hamilton, S. E. and Casey, D. (2016). Creation of a high spatio-temporal resolution global database of continuous mangrove forest cover for the 21st century (cgmfc-21). *Global Ecology and Biogeography*, 25(6):729–738.

Horstman, E., Dohmen-Janssen, C., Bouma, T., and Hulscher, S. (2015). Tidal-scale flow routing and sedimentation in mangrove forests: Combining field data and numerical modelling. *Geomorphology*, 228:244–262.

Horstman, E., Dohmen-Janssen, C., Narra, P., van den Berg, N., Siemerink, M., and Hulscher, S. (2014). Wave attenuation in mangroves: A quantitative approach to field observations. *Coastal Engineering*, 94:47–62.

Intergovernmental Panel on Climate Change (2022). *Sea Level Rise and Implications for Low-Lying Islands, Coasts and Communities*, page 321–446. Cambridge University Press.

Josten, M. (2024). Shorelinem, a new approach to 1d modeling of muddy coastlines.

Krone, R. B. (1962). Flume studies of the transport of sediment in estuarial shoaling processes; final report. *Hydraulic Engineering Laboratory and Sanitary Engineering Research Laboratory. Berkeley: University of California.*

Legay, A. (2020). Mudflat simulation: Adding the vegetation influence and its dynamics to an existing matlab model.

Lewis, R. R. (2005). Ecological engineering for successful management and restoration of mangrove forests. *Ecological Engineering*, 24(4):403–418. Wetland creation.

Mariotti, G. and Fagherazzi, S. (2010). A numerical model for the coupled long-term evolution of salt marshes and tidal flats. *Journal of Geophysical Research: Earth Surface*, 115(F1).

Michel, J. (2014). Oil spills in mangroves; planning & response considerations.

Ntriankos, V. (2021). The impact of extreme events on mudflats The Guyana case. Technical report, Delft University of Technology.

Partheniades, E. (1965). Erosion and deposition of cohesive soils. *Journal of the Hydraulics Division*, 91(1):105–139.

Robinet, A., Castelle, B., Idier, D., Harley, M., and Splinter, K. (2020). Controls of local geology and cross-shore/longshore processes on embayed beach shoreline variability. *Marine Geology*, 422:106118.

Roelvink, D. (2023). Adding mud coasts to shorelines. Powerpoint used for interal communication.

Roelvink, D., Huisman, B., Elghandour, A., Ghonim, M., and Reyns, J. (2020). Efficient modeling of complex sandy coastal evolution at monthly to century time scales. *Frontiers in Marine Science*, 7.

Rull, V. (2023). Rise and fall of caribbean mangroves. *Science of The Total Environment*, 885:163851.

Temmerman, S., Horstman, E. M., Krauss, K. W., Mullarney, J. C., Pelckmans, I., and Schoutens, K. (2023). Marshes and mangroves as nature-based coastal storm buffers. *Annual Review of Marine Science*, 15(1):95–118. PMID: 35850492.

van der Wegen, M., Roelvink, J. A., and Jaffe, B. E. (2019). Morphodynamic resilience of intertidal mudflats on a seasonal time scale. *Journal of Geophysical Research: Oceans*, 124(11):8290–8308.

van Maanen, B., Coco, G., and Bryan, K. R. (2015). On the ecogeomorphological feedbacks that control tidal channel network evolution in a sandy mangrove setting. *Proceedings. Mathematical, Physical, and Engineering Sciences / The Royal Society*, 471.

van Santen, P., Augustinus, P., Janssen-Stelder, B., Quartel, S., and Tri, N. (2007). Sedimentation in an estuarine mangrove system. *Journal of Asian Earth Sciences*, 29(4):566–575. Morphodynamics of the Red River Delta, Vietnam.

van Zelst, V. T. M., Dijkstra, J. T., and van Wesenbeeck, B. K. (2021). Cutting the costs of coastal protection by integrating vegetation in flood defences. *Nature Communications*, 12(6533).

Winterwerp, J., de Graaff, R., Groeneweg, J., and Luijendijk, A. (2007). Modelling of wave damping at guyana mud coast. *Coastal Engineering*, 54(3):249–261.

Xie, D., Schwarz, C., Kleinhans, M. G., Zhou, Z., and van Maanen, B. (2022). Implications of coastal conditions and sea-level rise on mangrove vulnerability: A bio-morphodynamic modeling study. *Journal of Geophysical Research: Earth Surface*, 127.

A Appendix

A.1 Model description ShorelineS

To model the coastal evolution of sandy coasts at a monthly to century time scale, the ShorelineS model is created in 2020. This model is specifically designed for sandy coasts and is a free form model that addresses the limitations of existing coastline models with fixed reference lines(Roelvink et al., 2020). ShorelineS is a line model, that has different strings of points along the coastline. These points can move on- and offshore depending on the active coastal profile. The model therefore avoids the complexities of grid-based approaches and geometrically complex volume reconstructions.

The ShorelineS model uses a [n,s]-coordinate system, where n is the cross-shore component and where s is the alongshore component, which is visible in figure 45. In this figure, ϕ_w is the angle of incidence of waves with respect to the North, ϕ_c is the orientation of the shore normal with respect to the coast, ϕ_{loc} is the local angle between waves and the normal to the shore (Roelvink et al., 2020), $Q_{s,i-1}$ is the incoming sand flux at a certain point, $Q_{s,i}$ is the outgoing sand flux at a certain point and x_i and y_i are determining the new positions of the shoreline (Roelvink et al., 2020).
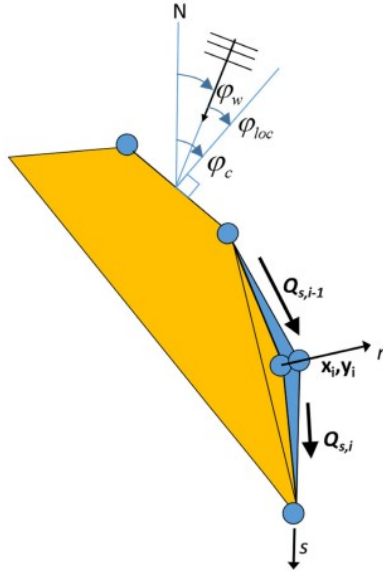

FIGURE 45: Topview of coastline set up in ShorelineS (Roelvink et al., 2020)

The basis for the model is the conservation of sediment before the coast, see Eq.(27) (Roelvink et al., 2020). In this equation, the coastline change over time ($\partial n/\partial t$) is determined by the longshore sediment transport (Q_s), the relative sea-level rise ($RSLR$) and the sources and sinks (q_i). The longshore transport and sources/ sinks are divided by the active profile height (D_c). The active profile height (approximately equal to the closure depth) can be determined with the significant wave height ($D_c \approx 9 * H_s$). The relative sea level rise is divided by $\tan \beta$, which is the average profile slope between the dune crest and the depth of closure (Roelvink et al., 2020).

$$\frac{\partial n}{\partial t} = -\frac{1}{D_c}\frac{\partial Q_s}{\partial s} - \frac{RSLR}{\tan \beta} + \frac{1}{D_c}\sum q_i \tag{27}$$

A.2   Model dynamics ShorelineM

Solution scheme for mud transport

The suspended sediment concentration C in the nearshore area A is solved implicitly by using a tridiagonal solution scheme. In the nearshore zone A, the longshore discharge (Q_i) is calculated by the wave- and wind forcing, mentioned in Eq.(4). The equations below show the solution scheme that is used, and determines the concentration at a cell C_i, based on the discharge Q_i at that location.

$$-\frac{Q_i}{\Delta s}C_{i-1} + \left(\frac{Q_{i+1}}{\Delta s} + wB\right)C_i = MB\frac{\tau_i - \tau_{cr}}{\tau_{cr}} + q_{riv} - q_m \; , \; Q_i > 0 \; \& \; Q_{i+1} > 0$$

$$\left(-\frac{Q_i}{\Delta s} + wB\right)C_i + \frac{Q_{i+1}}{\Delta s}C_{i+1} = MB\frac{\tau_i - \tau_{cr}}{\tau_{cr}} + q_{riv} - q_m \; , \; Q_i < 0 \; \& \; Q_{i+1} < 0$$

$$\left(\frac{Q_{i+1} - Q_i}{\Delta s} + wB\right)C_i = MB\frac{\tau_i - \tau_{cr}}{\tau_{cr}} + q_{riv} - q_m \; , \; Q_i < 0 \; \& \; Q_{i+1} > 0$$

$$-\frac{Q_i}{\Delta s}C_{i-1} + (wB)C_i + \frac{Q_{i+1}}{\Delta s}C_{i+1} = MB\frac{\tau_i - \tau_{cr}}{\tau_{cr}} + q_{riv} - q_m \; , \; Q_i > 0 \; \& \; Q_{i+1} < 0$$

Which can be rewritten in general form too:

$$a_i C_{i-1} + b C_i + c_i C_{i+1} = r_i \tag{28}$$

The longshore discharge (Q_i) is then used to calculate a fraction of the sediment at a previous location ($i-1$), the current location (i) and a next location ($i+1$), see Eq.(28) or the equations above.

These equations determine the direction of the longshore current and the possibility that a sediment particle is deposited (by multiplying the fall velocity w with the width of the nearshore zone B). In these equations and Eq.(28) the right hand side of the equation is defined as the sediment sinks and sources. Here the amount of sediment is determined based on the eroded sediment on locations where the shear stress τ exceeds the critical shear stress τ_{cr} ($MB\frac{\tau - \tau_{cr}}{\tau_{cr}}$), the sediment input through rivers ($q_{s,river}$) and the sediment output trough deposition in mangroves ($q_{s,mangroves}$). The amount of entrained sediment is increased with the erosion factor M.

With the values of a, b, and c in Eq.(28) and the sink- / source terms r_i, the suspended sediment concentration C is calculated, which is accomplished with a tridiagonal system, where the vectors a, b and c are the lower, main and upper diagonals and where r is the right-hand side. With the calculated concentration, the flux of sediment into the mangroves (q_m) is calculated by multiplying the fraction of sediment (calculated in Eq.(9)) with the actual concentration C, see Eq.(29).

$$q_m = q_{moverC}C \tag{29}$$

From Eq.(4) and the calculated sediment concentration C, the longshore sediment transport Q_s can be solved by using Eq.(30). In this equation the longshore sediment transport

is defined as the longshore discharge Q multiplied with the nearshore averaged sediment concentration $\bar{C}$.

$$Q_s = Q\bar{C} \tag{30}$$

With the longshore sediment transport Q_s and the space step ∂s, the longshore gradient of the sediment transport is calculated in Eq.(31).

$$\frac{\partial Q_s}{\partial s} = \frac{Q_s(i) - Q_s(i-1)}{\partial s \rho_s} \tag{31}$$

A.3 Model details of MFlat

A.3.1 Mangrove influence on the physical processes

The mangroves included in the model have influence on the following physical processes, that are given by the bullet-points below (Ntriankos, 2021):

- Increase the critical erosion shear stress

Critical shear stress increases linearly with the vegetation below-ground biomass (van Maanen et al., 2015; Mariotti and Fagherazzi, 2010).

$$\tau_{cr} = \tau_0(1 + K_{cr}\frac{W_{bg}}{W_{bg,max}}) \tag{32}$$

Where τ_0 is the critical shear stress without vegetation, K_{cr} is a dimensionless coefficient, W_{bg} is the below-ground biomass and $W_{bg,max}$ is the maximum below-ground biomass per grid cell in kg.

$$W_{bg,max} = 1.5N_{inf}W_{bg,tree} = 1.5\frac{0.9069dx^2}{\pi\left(10\sqrt{0.5\frac{D_{max}}{100}}\right)^2}1.28D_{max}^{1.17} \tag{33}$$

Where N_{inf} is the number of plants based on the competition stress, $W_{bg,tree}$ the below-ground biomass per tree and D_{max} the maximum mangrove diameter.

- Increase the drag coefficient

The drag coefficient $C_{D,veg}$ is increased based on a vegetation length scale L.

$$L = \frac{V_c - V_v}{A_v} \tag{34}$$

Where V_c is the control volume of a grid cell, V_v is the volume of the vegetation and A_v is the projected area of the vegetation.

$$C_{D,veg} = C_{D0} + \frac{e}{L} \tag{35}$$

Where C_{D0} is the initial drag coefficient (based on the input value of the Chezy friction factor) and $e = 5$ m.

- Increase of bed level by organic deposition

The bed level z is increased by organic deposition of the mangrove tress. The organic deposition follows from the biomass:

$$Z_{org} = K_{org} \frac{W_{bg}}{W_{bg,max}} \tag{36}$$

Where K_{org} is a organic deposition coefficient and W_{bg} is the below-ground biomass.

- Reduction of wave impact

The reduction of wave impact due to vegetation (D_v) is added by the total wave energy balance:

$$\frac{dEc_g}{dx} = S_w - D_b - D_f - D_v \tag{37}$$

This dissipation of energy due to vegetation is defined in the following way:

$$D_v = \frac{1}{2\sqrt{\pi}} \rho \hat{C}_D D \frac{N}{dx^2} \left(\frac{kg}{2\omega} \right)^3 \frac{sinh^3(kH_{uw}) + 3sinh(kH_{uw})}{3kcosh^3(kh)} H_{rms}^3 \tag{38}$$

Where ρ is the water density, $\hat{C}_d$ is the modified drag coefficient, D is the mangrove diameter, N is the number of plants, k is the angular wave number, g the gravity acceleration, ω the angular wave frequency, h is the water depth, H_{uw} is the vegetation height under water and H_{rms} is the root-mean square wave height.

A.3.2 Cross-shore profiles MFlat

Wave height of 0.10 meter
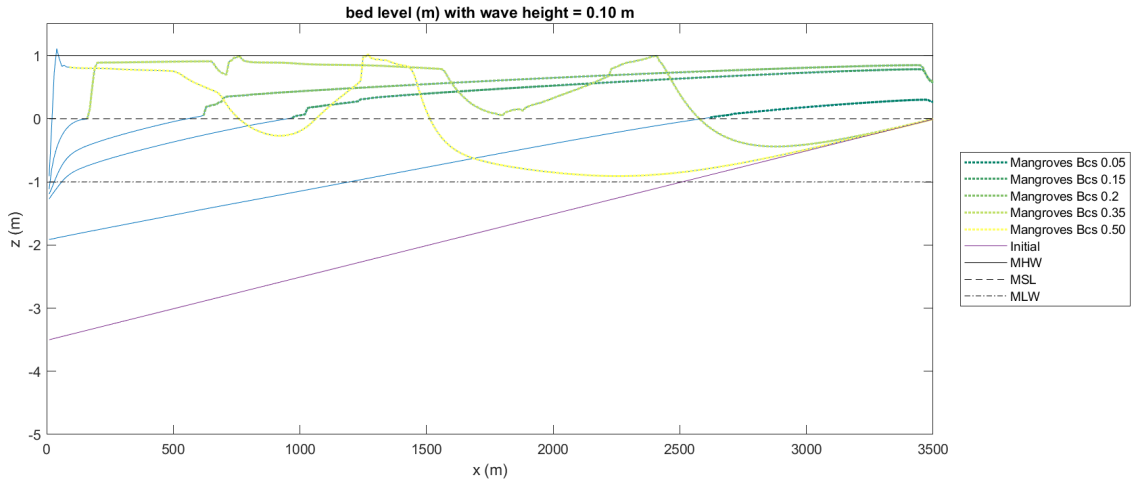
FIGURE 46: Cross-shore profiles of different simulations in MFlat with a wave height H_{rms} of 0.10 m and different boundary sediment concentrations c_{bcs}

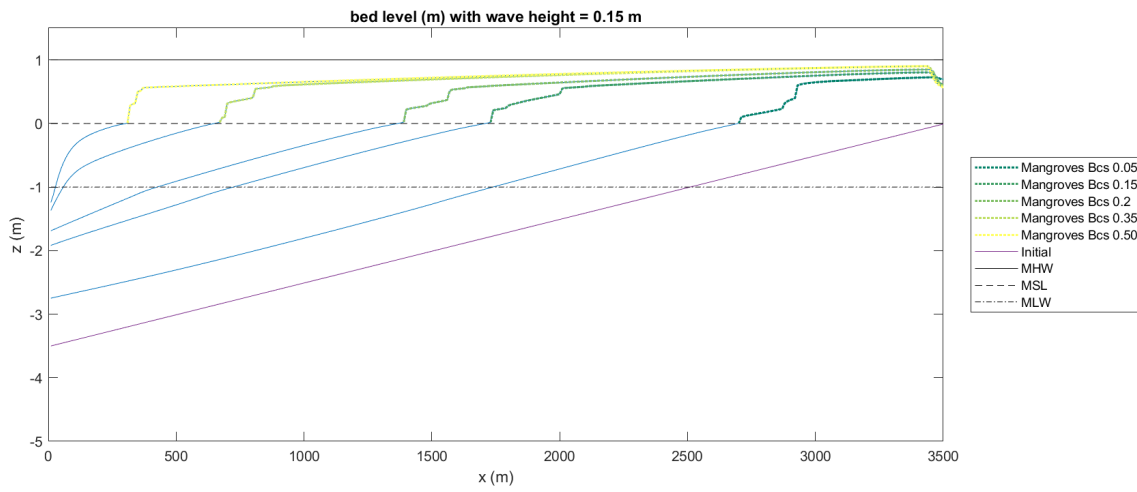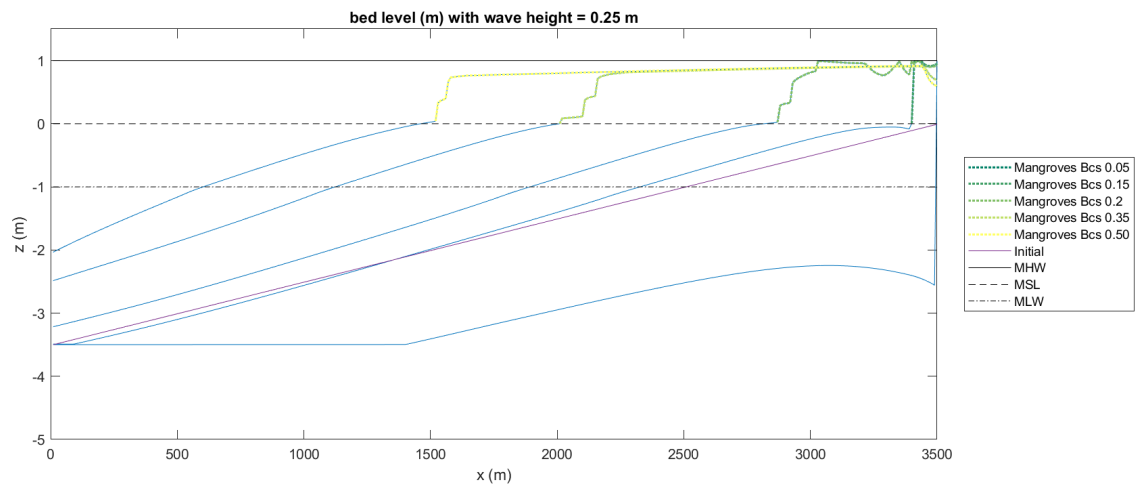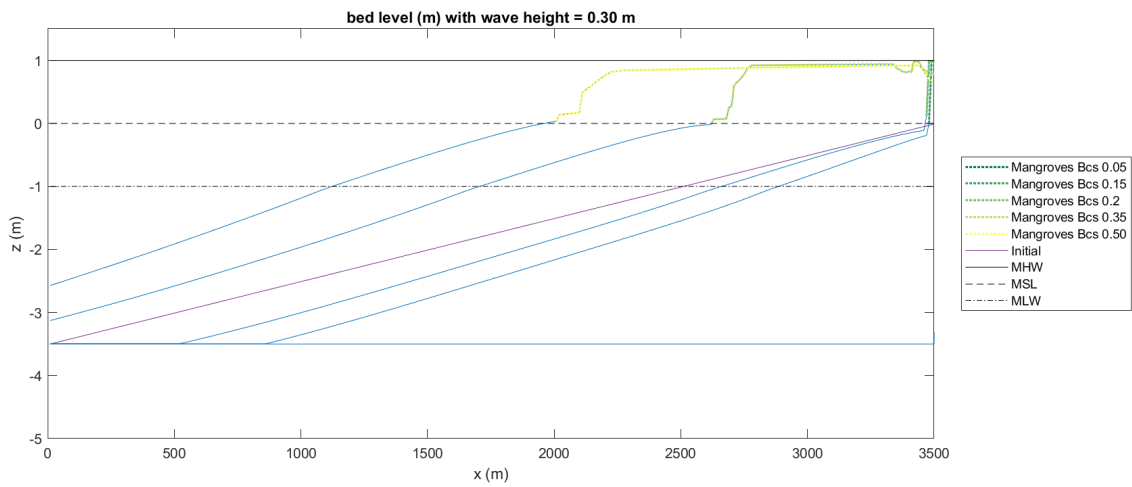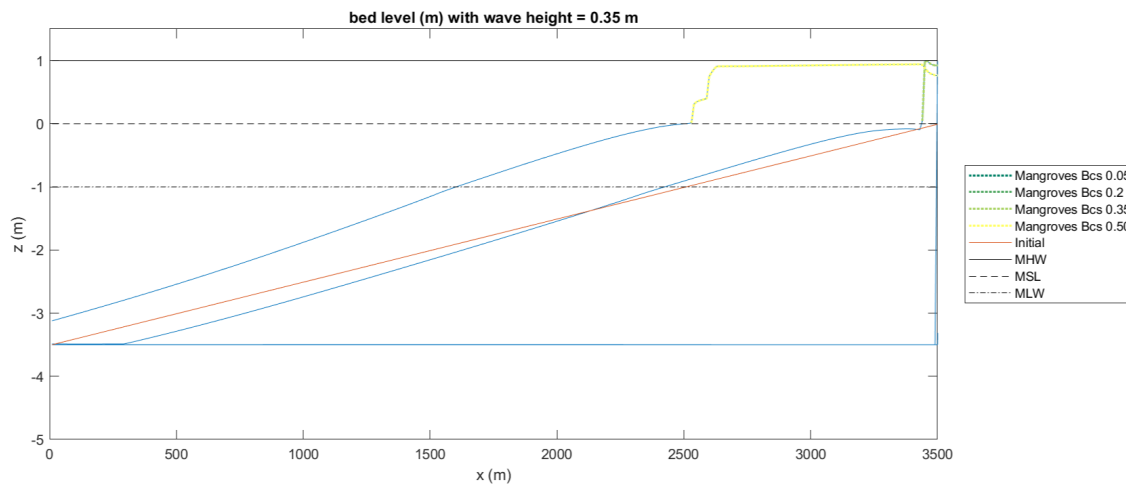**Wave height of 0.15 meter**

FIGURE 47: Cross-shore profiles of different simulations in MFlat with a wave height H_{rms} of 0.15 m and different boundary sediment concentrations c_{bcs}

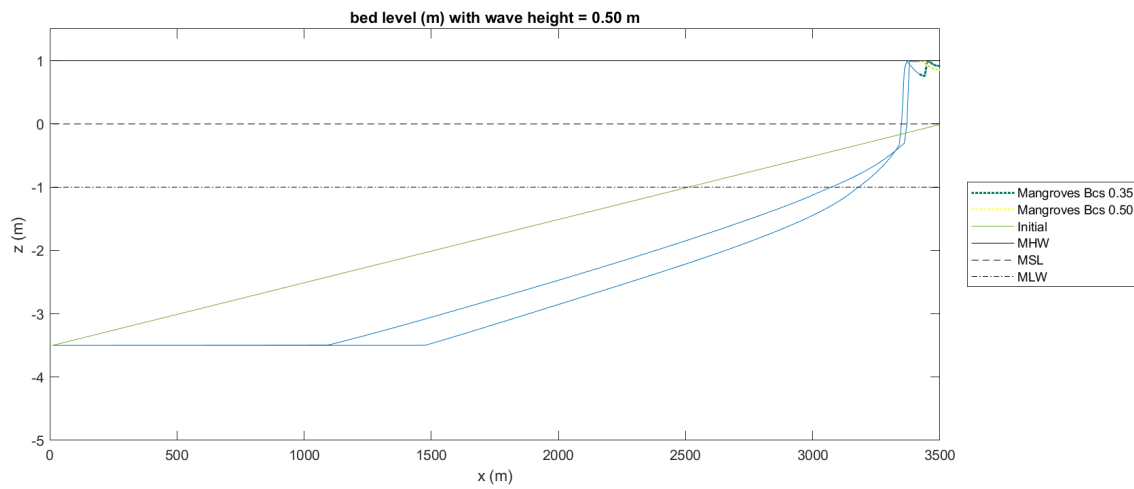**Wave height of 0.25 meter**

FIGURE 48: Cross-shore profiles of different simulations in MFlat with a wave height H_{rms} of 0.25 m and different boundary sediment concentrations c_{bcs}

Wave height of 0.30 meter

FIGURE 49: Cross-shore profiles of different simulations in MFlat with a wave height H_{rms} of 0.30 m and different boundary sediment concentrations c_{bcs}

Wave height of 0.35 meter

FIGURE 50: Cross-shore profiles of different simulations in MFlat with a wave height H_{rms} of 0.35 m and different boundary sediment concentrations c_{bcs}

Wave height of 0.50 meter

FIGURE 51: Cross-shore profiles of different simulations in MFlat with a wave height H_{rms} of 0.50 m and different boundary sediment concentrations c_{bcs}

A.3.3 Sediment trapping efficiency

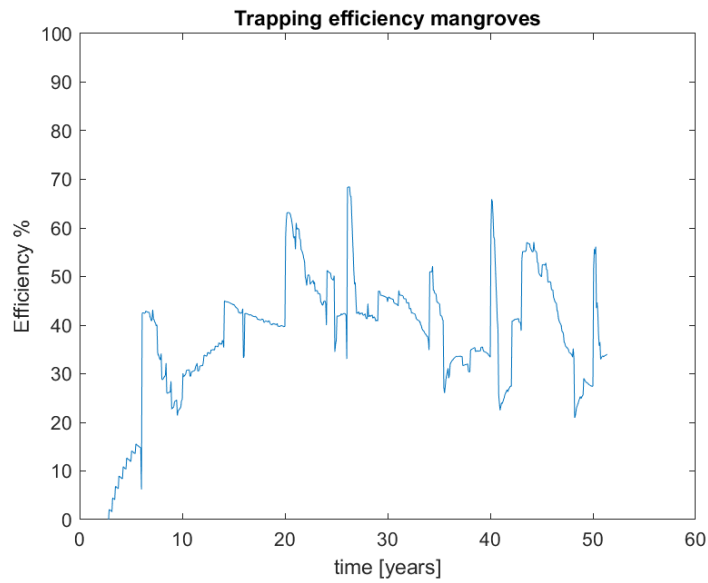**Wave height of 0.15 meter, boundary sediment concentration of 0.05 g/l**

FIGURE 52: Sediment trapping efficiency over time for a wave height H_{rms} of 0.15 m and a boundary sediment concentration c_{bcs} of 0.05 g/l.

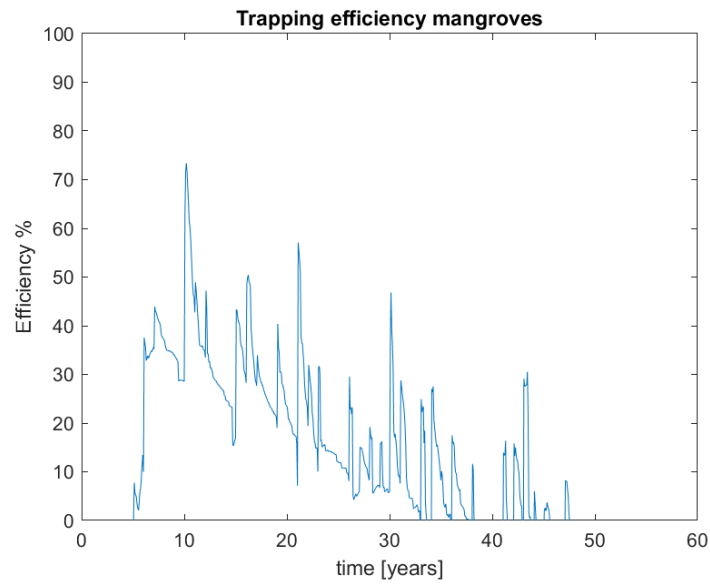**Wave height of 0.25 meter, boundary sediment concentration of 0.35 g/l**

FIGURE 53: Sediment trapping efficiency over time for a wave height H_{rms} of 0.25 m and a boundary sediment concentration c_{bcs} of 0.35 g/l.

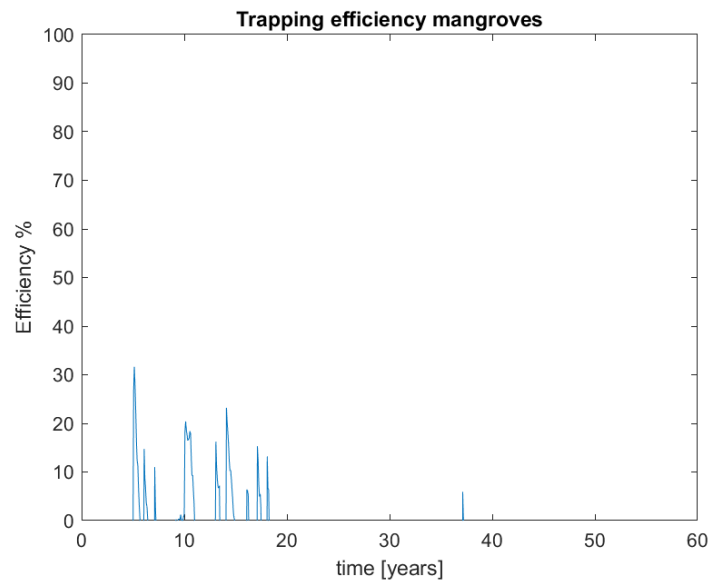**Wave height of 0.35 meter, boundary sediment concentration of 0.50 g/l**

FIGURE 54: Sediment trapping efficiency over time for a wave height H_{rms} of 0.35 m and a boundary sediment concentration c_{bcs} of 0.50 g/l.

A.3.4 Tidal prism MFlat
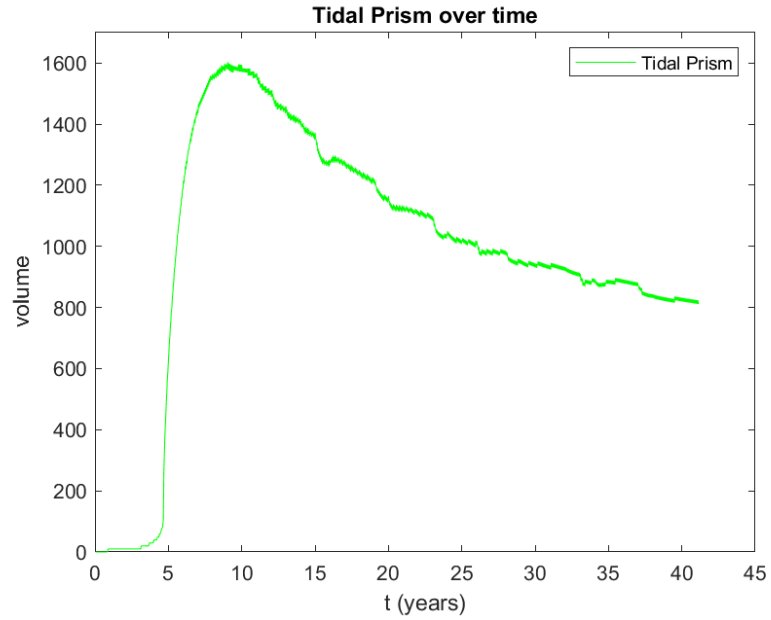
Tidal prism over time

FIGURE 55: Tidal prism development over time for a wave height H_{rms} of 0.15 m and a boundary sediment concentration c_{bcs} of 0.50 g/l.